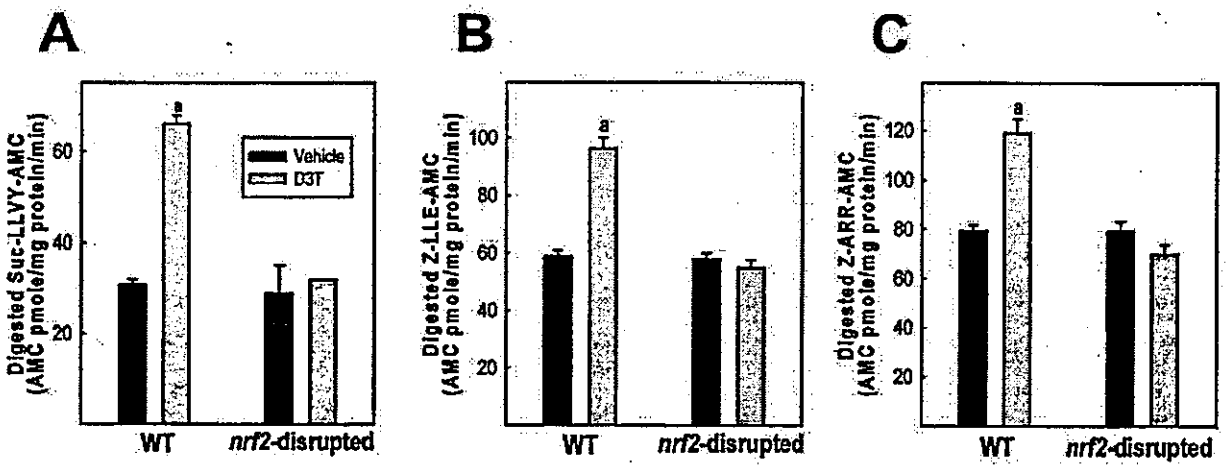

FIG. 3. Enhanced peptidase activities of proteasomes in wild-type mouse liver following treatment with D3T. Chemoptypsin-like (Suc-LLVY) (A), postglutamic (Z-LLE) (B), and trypsin-like (Z-ARR) (C) peptidase activities in liver homogenates prepared from wild-type and *nrf2*-disrupted mice were measured. Values are means ± standard errors from three experiments. a, $P < 0.05$ compared with vehicle-treated control group.

AREs are followed or preceded by inverted ARE-like sequences. Promoter truncation analysis was performed to identify the functional AREs from this promoter. The full-length promoter (−3.4kb-luc) was truncated in five different constructs, and luciferase activities from these constructs in murine embryonic fibroblasts from wild-type mice following sulforaphane treatment or Nrf2 overexpression were measured (Fig. 5A). The full-length (−3.4kb-luc) promoter was activated by sulforaphane treatment (1.5-fold), as well as by Nrf2 overexpression (2.5-fold) (Fig. 5B). Responses to sulforaphane and Nrf2 were higher (three- to fourfold) in proximal promoter constructs (−1.1kb-luc and −0.5kb-luc) than in the full-length promoter. When the proximal promoter region (−1.1 kb to −1 bp) was deleted from the full-length promoter, the resulting construct was not activated by sulforaphane treatment or Nrf2 expression [−3.4-del (−1.1)-luc]. These results suggest that a promoter containing 0.5 kb upstream of the start codon can be activated by the Nrf2-ARE pathway (Fig. 5B). However, deletion of either one of these tandem AREs [−0.2kb-luc and −0.5kb-del (−0.2)-luc] largely abolished the responses to sulforaphane and Nrf2, indicating that these two tandem AREs are necessary for the full activation of the *PSMB5* promoter by Nrf2-ARE signaling. The response of the proximal promoter of PSMB5 (−1.1kb-luc) was also measured following treatment with different antioxidants (Fig. 6A). Luciferase activity driven by the proximal promoter in wild-type cells was elevated following treatment with these antioxidants in a pattern similar to that of the induced changes in mRNA levels (Fig. 4). Sulforaphane showed the highest activation of this promoter (2.9-fold), and this activation was largely attenuated when the reporter was transfected into *nrf2*-disrupted cells (Fig. 6A). Expression of excess amounts of MafK, a repressor binding partner of Nrf2, suppressed basal promoter activity by 50% and completely blocked promoter activation by overexpression of Nrf2, as seen with other promoters regulated by AREs (32) (Fig. 6B). The enhanced constitutive promoter activity in *keap1*-disrupted cells (9.4-fold; Fig. 6B) also indicated that the promoter of *PSMB5* is regulated by Nrf2. Nrf2 accumulates in the nuclei of *keap1*-disrupted cells, leading to high basal expression of ARE-regulated genes, such as that encoding

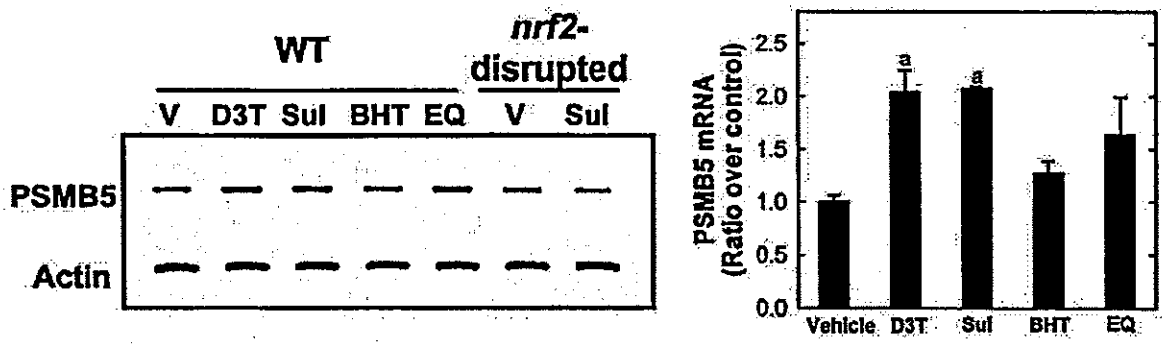

FIG. 4. Effect of antioxidants on the level of PSMB5 transcripts in murine embryonic fibroblasts. Transcript levels for *PSMB5* were measured following treatment with antioxidants D3T (30 μM), sulforaphane (Sul; 10 μM), butylhydroxytoluene (BHT; 100 μM), and ethoxyquin (EQ; 80 μM) for 18 h in fibroblasts from wild-type and *nrf2*-disrupted mice. The histogram depicts the means ± standard errors from three separate experiments. a, $P < 0.05$ compared with vehicle-treated controls.

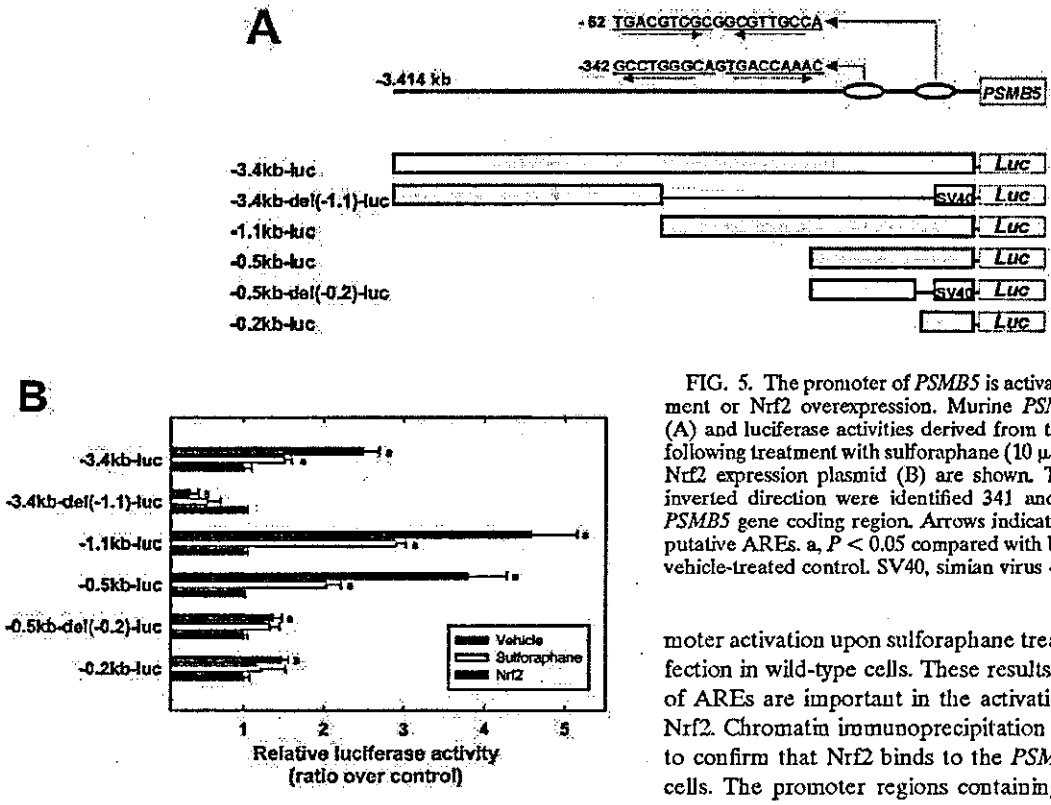

FIG. 5. The promoter of *PSMB5* is activated by sulforaphane treatment or Nrf2 overexpression. Murine *PSMB5* promoter constructs (A) and luciferase activities derived from these truncated promoters following treatment with sulforaphane (10 μM) or cotransfection of an Nrf2 expression plasmid (B) are shown. Two tandem AREs in an inverted direction were identified 341 and 52 bp upstream of the *PSMB5* gene coding region. Arrows indicate the orientation of these putative AREs. a, $P < 0.05$ compared with blank plasmid-transfected, vehicle-treated control. SV40, simian virus 40.

NQO1 (44a). Collectively, these results indicate that expression of proteasome catalytic subunit PSMB5 is elevated by the Nrf2 pathway.

PSMB5 is regulated by tandem AREs located in its proximal promoter. To confirm the results from promoter truncation, the tandem AREs were mutated. Mutations in either the −341 ARE or −52 ARE partially affected inducer responses (Fig. 7), while mutations in both tandem AREs largely abolished promoter activation upon sulforaphane treatment or Nrf2 cotransfection in wild-type cells. These results indicate that both sets of AREs are important in the activation of the promoter by Nrf2. Chromatin immunoprecipitation assays were performed to confirm that Nrf2 binds to the *PSMB5* promoter in intact cells. The promoter regions containing tandem AREs at kb −341 and −52 were detected by PCR amplification with Nrf2-immunoprecipitated chromatin from sulforaphane-treated, wild-type cells (Fig. 8A). As a positive control, the ARE of the *GSTA1* promoter, which is a well-characterized functional ARE (14), was detected in Nrf2-immunoprecipitated samples, but not in immunoprecipitants with nonspecific immunoglobulin G or GATA-1. The β-actin and *GATA-1* promoters were not amplified by the same number of PCR cycles in Nrf2-immunoprecipitated samples. Levels of binding of Nrf2 to the *PSMB5* promoter were higher in sulforaphane-treated wild-

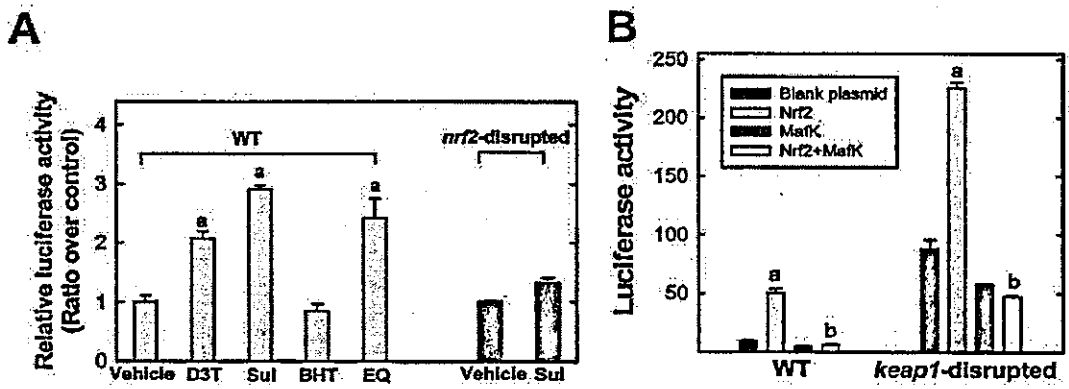

FIG. 6. The promoter of *PSMB5* is regulated by the Nrf2-ARE pathway. (A) Luciferase activity driven by the proximal *PSMB5* promoter (−1.1kb-luc) following treatment with antioxidants in wild-type and *nrf2*-disrupted cells. BHT, butylhydroxytoluene; EQ, ethoxyquin. (B) Elevated basal activity of the proximal *PSMB5* promoter (−1.1kb-luc) in *keap1*-disrupted cells. Overexpression of MafK inhibited promoter activation by Nrf2. a, $P < 0.05$ compared with blank plasmid-transfected, vehicle-treated control; b, $P < 0.05$ compared with pcDNA3-Nrf2-transfected group. WT, wild type.

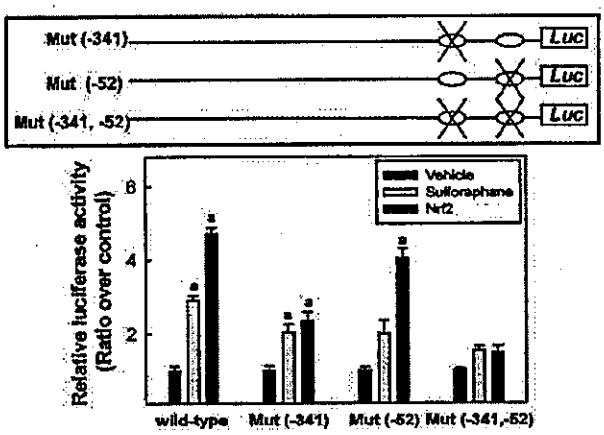

FIG. 7. Response of mutated *PSMB5* promoter to sulforaphane (Sul) treatment and Nrf2 overexpression in wild-type cells. AREs located at −341 and −52 were mutated, and singly and doubly mutated promoters were generated from the proximal promoter construct (−1.1kb-luc). Values are means ± standard errors from three experiments. a, $P < 0.05$ compared with blank plasmid-transfected, vehicle-treated control.

type cells than in vehicle-treated cells. A similar pattern of binding was observed with the *GSTA1* ARE (Fig. 8B). The *GSTA1* ARE and *PSMB5* promoters were also amplified from Nrf2-bound chromatin from *keap1*-disrupted cells, but not from *nrf2*-disrupted cells.

DISCUSSION

Oxidative stress contributes to aging and age-related diseases such as cancer, cardiovascular disease, chronic inflammation, and neurodegenerative diseases. Levels of oxidized proteins, phospholipids, and DNA increase in these processes (40). There is abundant evidence that oxidized low-density lipoprotein is involved in the formation of atherosclerotic lesions (18). Accumulation and aggregation of abnormal proteins are common features of neurodegenerative diseases; levels of oxidized and nitrated amino acids in Parkinson's and Alzheimer's diseases are high (15, 17, 34). Reduced expression of proteasome components and inhibition of proteolytic activity appear to be primary events leading to neuronal death during aging and neurodegenerative diseases (8, 17, 22). Antioxidants can prevent or retard many of the manifestations of oxidative damage. Direct antioxidants inactivate free radicals, and cell-based and animal studies demonstrate that vitamins C, E, and β-carotene are effective in preventing oxidative injury (9). Epidemiological studies have shown that consumption of diets rich in vegetables and fruits, which are excellent sources of antioxidants, are associated with reduced cancer incidence and that dietary intake of vitamin E is associated with lower risk of coronary disease (41). Paradoxically though, it has been difficult to recapitulate the protective benefits of these diets in clinical trials with defined antioxidant interventions (16). Vegetable-rich diets are also an abundant source of indirect antioxidants that, although they cannot scavenge free radicals, enhance the antioxidative capacity of cells (10). These phytochemicals increase intracellular levels of the antioxidant glutathione, boost synthesis of reducing equivalents such as NADPH, and increase the expression of enzymes, such as glutathione *S*-transferase and NQO1, that detoxify chemicals poised to generate oxidants. Indirect antioxidants can be classified into at least nine chemically distinct categories, including isothiocyanates (e.g., sulforaphane) and dithiolethiones (e.g., D3T), that nonetheless have the common chemical property of reactivity with sulfhydryl groups (10). In a few instances, exemplified by phenolic antioxidants used as food additives and polyphenols found in foods and teas, some agents can dually function as direct and indirect antioxidants (10). Many animal studies now indicate that indirect antioxidants of both natural and synthetic origin can prevent carcinogenesis, although their effects against other chronic diseases associated with aging are largely unexplored. Clinical trials have demonstrated that oltipraz, a synthetic analog of D3T, inhibits some of the early actions of the hepatocarcinogen aflatoxin B_1 while another drug, anethole dithiolethione, reduces the extent of bronchial dysplasia in smokers (28, 45). In animal models the protective actions of dithiolethiones and sulforaphane depend on the Nrf2 signaling pathway. Disruption of *nrf2* largely inhibits the induction of protective genes by these

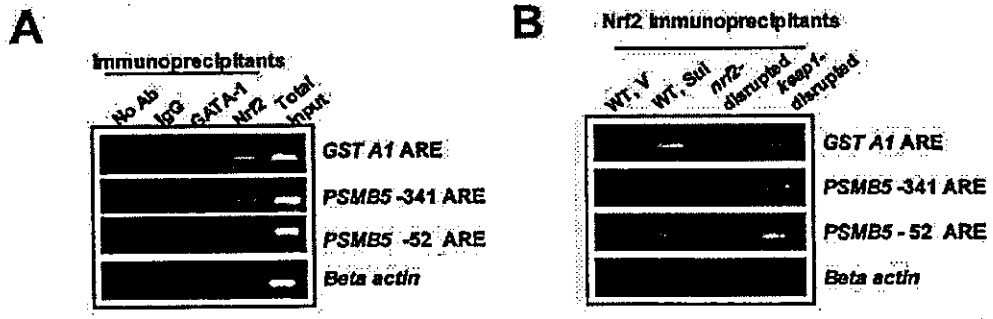

FIG. 8. Binding of Nrf2 to *PSMB5* promoter in intact cells. (A) Chromatin immunoprecipitants with no antibody (Ab), immunoglobulin G (IgG), GATA-1, or Nrf2 were used for PCR amplification of each promoter. ARE-containing promoter regions from *PSMB5* and the *GSTA1* promoter were detected in Nrf2 immunoprecipitants obtained from sulforaphane-treated wild-type cells. (B) Enhanced binding of Nrf2 to the *PSMB5* promoter following sulforaphane (Sul) treatment compared to that in vehicle (V)-treated cells. Promoter regions of *GSTA1* and *PSMB5* genes were detected in Nrf2-immunoprecipitants from *keap1*-disrupted cells, but not *nrf2*-disrupted cells. WT, wild type.

antioxidants, with resultant loss of protective efficacy against chemical carcinogenesis (25, 35, 43).

Nrf2 is a central molecular target of indirect antioxidants, and products of the genes downstream of *nrf2* are a key mammalian defense system that enables adaptation to stresses and promotes cell survival. Genes now recognized as being under the regulation of the Nrf2-ARE signaling pathway include a panel of genes encoding xenobiotic conjugating enzymes, enzymes that provide cofactors (glutathione) and reducing equivalents (NADPH) for these reactions, and antioxidative enzymes and proteins (27, 43). In this study, we demonstrate that the genes forming the 26S proteasome complex are coordinately regulated by Nrf2 in the response to indirect antioxidants. Dithiolethiones elevated transcript levels for 24 out of the 34 subunits that constitute the 26S proteasome in mouse liver; 19 out of these 24 subunits were increased in wild-type mice but not in *nrf2*-disrupted mice. Concordantly, protein levels and proteolytic activities were elevated by D3T only in wild-type mice. Promoter truncation, mutation, and chromatin immunoprecipitation studies of the murine *PSMB5* gene, which has a chemotrypsin-like proteolytic activity, further support the critical role of the Nrf2-ARE signaling pathway in the regulation of these genes.

The consensus sequence of the ARE has been proposed to be TGA(C/T)NNNGC. The first three bases from the 5′ direction are known to be critical for its activity, and the GC box is needed for maximal function (46). The ARE was identified in the promoter region of multiple phase 2 genes, and AREs from rat, mouse, and human *NQO1*, mouse and rat *GSTA1*, and human γ-glutamylcysteine ligases, are well-characterized, functional AREs. Mouse *GSTA1* has repeated AREs (underlined) in a forward direction (ATGAC ATTGCTAATGGTGACAAAGCA), and rat *NQO1* has also tandem AREs in an inverted direction (CTAGAGTCAC AGTGACTTGGCA) (12, 14, 33). One of the AREs from NQO1 contains the complete consensus sequence of the ARE, while the other has no GC box. Both elements of the tandem AREs of *GSTA1* and *NQO1* are essential for the response of these promoters to enzyme inducers and Nrf2 expression (14, 33). By contrast, human γ-glutamylcysteine ligases have a single functional ARE (TGACAAGC in the regulatory subunit and TGAC TCAGC in the catalytic subunit) in their promoters (33). The murine *PSMB5* gene has tandem AREs in an inverted direction that are similar to the rat *NQO1* ARE. From the results of promoter truncation and mutation analyses, the two tandem AREs in the *PSMB5* promoter appear to be important for the maximal response of this promoter to Nrf2-mediated signaling. Many other subunits of the murine proteasome have putative AREs in their 5′-flanking region. In addition, the promoters of rat and human *PSMB5* have several ARE motifs. Levels of protein PSMB5 in rat tissues can also be elevated following treatment with D3T (data not shown).

The ubiquitin-proteasome pathway maintains cellular homeostasis by regulating proteins involved in signaling and cell cycle pathways. Nrf2 is a substrate for the ubiquitin-proteasome system. Treatment of cells with a proteasome inhibitor prevents rapid degradation of this protein, leading to enhanced expression of the downstream gene encoding γ-glutamylcysteine ligase (37). Recently, Itoh et al. (21) proposed that Nrf2 protein turnover is regulated by Keap1-mediated subcellular compartmentalization of this transcription factor. In our study, D3T induced the expression of a broad range of proteasome subunits encompassing both the catalytic core (20S proteasome) and the ATP-dependent regulatory core (19S proteasome). Twelve out of 14 of the subunits of the 20S proteasome were induced. By contrast, D3T increased the expression of just a few of the ubiquitination enzymes in mouse liver (27). Many studies have demonstrated that the 20S proteasome can directly degrade oxidatively damaged proteins without assistance from the ubiquitination process by direct recognition of a hydrophobic patch derived from oxidation (6). Mutational inactivation of the E1 ubiquitin-activating enzyme does not affect the degradation of oxidized proteins by proteasomes. Therefore, the enhanced expression of multiple subunits of the 26S proteasome, and in particular its 20S catalytic core, by antioxidants might facilitate the removal of damaged proteins, without disturbing physiologic regulation of other proteins. This action may function to attenuate or perhaps prevent progression of human diseases related to oxidative stress damage. Expression of β-subunits of the proteasome is repressed during aging, and this is reflected in increased levels of oxidized and ubiquitinated proteins within cells. A recent report has shown that proteasome expression in senescent cells is downregulated and that stable expression of PSMB5 by transfection reversed the phenotype of senescence and led to enhanced resistance to oxidative stresses (5).

Regulation of the mammalian proteasome is not well understood. Direct oxidative modification of the catalytic core subunits of the proteasome inhibits their activities (7). There are few reports concerning the regulation of expression of proteasome subunits in mammalian cells. Immunoproteasomes are inducible by chemical treatment in animal cells. Expression of PSMB8, PSMB9, and PSMB10 is enhanced by gamma interferon and lipopolysaccharide exposure (13, 48). Takabe et al. (42) reported that the antiatherogenic antioxidant probucol repressed expression of PSMA2, PSMA3, and PSMA4. Lee et al. (29) showed that overexpression of the antiapoptotic protein BCL-2 increased proteasome activity in animal cells. Very recently, Meiners et al. (31) demonstrated that the proteasome inhibitor MG132 increases the expression of a broad range of subunits of the proteasome in mammalian cells. In *Saccharomyces cerevisiae*, expression of the 26S proteasome subunits is coordinately regulated by the transcription factor Rpn4p (30, 47). Rpn4p is a C_2H_2-type finger motif protein that regulates basal expression of yeast proteasome subunits by transactivating proteasome-associated control elements (5′-GGTGGCAA A-3′) in their promoters. Expression of this protein can be upregulated by Pdr1p and Yap1p under conditions of stress. While Nrf2 appears to be a universal transcription factor for the upregulation of proteasome subunits by antioxidants in mammalian cells, Nrf2 and Rpn4p have no apparent homology.

Collectively, our results indicate that the 26S proteasome is one of several target gene categories regulated by the transcription factor Nrf2 that can contribute to protection against oxidative stress. Induction of these protective pathways provides efficient means for cells to survive conditions of stress that result from endogenous processes (e.g., inflammation) or exogenous ones (e.g., environmental pollutants) that collec-

tively enhance the burden of chronic disease. Induction of these pathways by indirect antioxidants through dietary or pharmacological means provides opportunities for broad-ranging protection in settings where supplementations with direct antioxidants have had limited benefit.

ACKNOWLEDGMENTS

This work was supported by grants CA39416 and CA94076 from the National Institutes of Health and Center grant ES03819.

REFERENCES

1. **Almond, J. B., and G. M. Cohen.** 2002. The proteasome: a novel target for cancer chemotherapy. Leukemia 16:433–443.
2. **Aoki, Y., H. Sato, N. Nishimura, S. Takahashi, K. Itoh, and M. Yamamoto.** 2001. Accelerated DNA adduct formation in the lung of the Nrf2 knockout mouse exposed to diesel exhaust. Toxicol. Appl. Pharmacol. 173:154–160.
3. **Chan, K., X. D. Han, and Y. W. Kan.** 2001. An important function of Nrf2 in combating oxidative stress: detoxification of acetaminophen. Proc. Natl. Acad. Sci. USA 98:4611–4616.
4. **Cho, H.-Y., A. E. Jedlicka, M. S. Sekhar, P. M. Reddy, L. Y. Zhang, T. W. Kensler, M. Yamamoto, and S. R. Kleeberger.** 2001. Linkage analysis of susceptibility to hyperoxia: Nrf2 is a candidate gene. Am. J. Respir. Cell Mol. Biol. 26:42–51.
5. **Chondrogianni, N., F. L. Stratford, I. P. Trougakos, B. Friguet, A. J. Rivett, and E. S. Gonos.** 2003. Central role of the proteasome in senescence and survival of human fibroblasts: induction of a senescence-like phenotype upon its inhibition and resistance to stress upon its activation. J. Biol. Chem. 278:28026–28037.
6. **Davies, K. J.** 2001. Degradation of oxidized proteins by the 20S proteasome. Biochimie 83:301–310.
7. **Demasi, M., G. M. Silva, and L. E. Netto.** 2003. 20 S proteasome from *Saccharomyces cerevisiae* is responsive to redox modifications and is S-glutathionylated. J. Biol. Chem. 278:679–685.
8. **Ding, Q., and J. N. Keller.** 2001. Proteasomes and proteasome inhibition in the central nervous system. Free Radic. Biol. Med. 31:574–584.
9. **Evans, P., and B. Halliwell.** 2001. Micronutrients: oxidant/antioxidant status. Br. J. Nutr. 85:S67–S74.
10. **Fahey, J. W., and P. Talalay.** 1999. Antioxidant functions of sulforaphane: a potent inducer of phase II detoxication enzymes. Food Chem. Toxicol. 37: 973–979.
11. **Fahey, J. W., X. Haristoy, P. M. Dolan, T. W. Kensler, I. Scholtus, K. K. Stephenson, P. Talalay, and A. Lozniewski.** 2002. Sulforaphane inhibits extracellular, intracellular, and antibiotic-resistant strains of *Helicobacter pylori* and prevents benzo[*a*]pyrene-induced stomach tumors. Proc. Natl. Acad. Sci. USA 99:7610–7615.
12. **Favreau, L., and C. B. Pickett.** 1995. The rat quinone reductase antioxidant response element: identification of the nucleotide sequence required for basal and inducible activity and detection of antioxidant response element-binding proteins in hepatoma and non-hepatoma cell lines. J. Biol. Chem. 270:24468–24474.
13. **Foss, G. S., F. Larsen, J. Solheim, and H. Prydz.** 1998. Constitutive and interferon-gamma-induced expression of the human proteasome subunit multicatalytic endopeptidase complex-like 1. Biochim. Biophys. Acta 1402: 17–28.
14. **Friling, R. S., A. Bensimon, Y. Tichauer, and V. Daniel.** 1990. Xenobiotic-inducible expression of murine glutathione S-transferase Ya subunit gene is controlled by an electrophile-responsive element. Proc. Natl. Acad. Sci. USA 87:6258–6262.
15. **Glickman, M. H., and A. Ciechanover.** 2002. The ubiquitin-proteasome proteolytic pathway: destruction for the sake of construction. Physiol. Rev. 82:373–428.
16. **Halliwell, B.** 2000. The antioxidant paradox. Lancet 355:1179–1180.
17. **Halliwell, B.** 2002. Hypothesis: proteasomal dysfunction: a primary event in neurogeneration that leads to nitrative and oxidative stress and subsequent cell death. Ann. N. Y. Acad. Sci. 962:182–194.
18. **Heinecke, J. W.** 1998. Oxidants and antioxidants in the pathogenesis of atherosclerosis: implications for the oxidized low density lipoprotein hypothesis. Atherosclerosis 141:1–15.
19. **Itoh, K., T. Chiba, S. Takahashi, T. Ishii, K. Igarashi, Y. Katoh, T. Oyake, N. Hayashi, K. Satoh, I. Hatayama, M. Yamamoto, and Y. Nabeshima.** 1997. An Nrf2/small Maf heterodimer mediates the induction of phase II detoxifying enzyme gene through antioxidant response elements. Biochem. Biophys. Res. Commun. 236:313–322.
20. **Itoh, K., N. Wakabayashi, Y. Katoh, T. Ishii, K. Igarashi, J. D. Engel, and M. Yamamoto.** 1999. Keap1 represses nuclear activation of antioxidant responsive elements by Nrf2 through binding to the amino-terminal Neh2 domain. Genes Dev. 13:76–86.
21. **Itoh, K., N. Wakabayashi, Y. Katoh, T. Ishii, T. O'Connor, and M. Yamamoto.** 2003. Keap1 regulates both cytoplasmic-nuclear shuttling and degradation of Nrf2 in response to electrophiles. Genes Cells 8:379–391.
22. **Jenner, P.** 2003. Oxidative stress in Parkinson's disease. Am. Neurol. 53: 526–538.
23. **Jirousek, L., and J. Starka.** 1958. Uber das vorkommen von trithionen (1,2-dithiacyclopent-4-en-3-thione) in brassicapflanzen. J. Natwiss. 45:386–387.
24. **Kensler, T. W., J. D. Groopman, T. R. Sutter, T. J. Curphey, and B. D. Roebuck.** 1999. Development of cancer chemopreventive agents: oltipraz as a paradigm. Chem. Res. Toxicol. 12:113–126.
25. **Kwak, M.-K., K. Itoh, M. Yamamoto, T. R. Sutter, and T. W. Kensler.** 2001. Role of transcription factor Nrf2 in the induction of hepatic phase 2 and antioxidative enzymes in vivo by the cancer chemoprotective agent, 3*H*-1,2-dithiole-3-thione. Mol Med. 7:135–145.
26. **Kwak, M.-K., K. Itoh, M. Yamamoto, and T. W. Kensler.** 2002. Enhanced expression of the transcription factor Nrf2 by cancer chemopreventive agents: role of antioxidant response element-like sequences in the *nrf2* promoter. Mol. Cell. Biol. 22:2883–2892.
27. **Kwak, M.-K., N. Wakabayashi, K. Itoh, H. Motohashi, M. Yamamoto, and T. W. Kensler.** 2003. Modulation of gene expression by cancer chemopreventive dithiolethiones through the Keap1-Nrf2 pathway: identification of novel gene clusters for cell survival. J. Biol. Chem. 278:8135–8145.
28. **Lam, S. A., C. MacAulay, J. C. Le Riche, Y. Dyachkova, A. Coldman, M. Guillaud, E. Hawk, M. O. Christen, and A. F. Gazdar.** 2002. A randomized phase IIb trial of anethole dithiolethione in smokers with bronchial dysplasia. J. Natl. Cancer Inst. 94:1001–1009.
29. **Lee, M., D. H. Hyun, K. A. Marshall, L. M. Ellerby, D. E. Bredesen, P. Jenner, and B. Halliwell.** 2001. Effect of overexpression of BCL-2 on cellular oxidative damage, nitric oxide production, antioxidant defenses, and the proteasome. Free Radic. Biol. Med. 31:1550–1559.
30. **Mannhaupt, G., R. Schnall, V. Karpov, I. Vetter, and H. Feldmann.** 1999. Rpn4p acts as a transcription factor by binding to PACE, a nonamer box found upstream of 26S proteasomal and other genes in yeast. FEBS Lett. 450:27–34.
31. **Meiners, S., D. Heyken, A. Weller, A. Ludwig, K. Stangl, P. M. Kloetzel, and E. Kruger.** 2003. Inhibition of proteasome activity induces concerted expression of proteasome genes and de novo formation of mammalian proteasomes. J. Biol. Chem. 278:21517–21525.
32. **Motohashi, H., T. O'Connor, F. Katsuoka, J. D. Engel, and M. Yamamoto.** 2002. Integration and diversity of the regulatory network composed of Maf and CNC families of transcription factors. Gene 294:1–12.
33. **Nguyen, T., H. C. Huang, and C. B. Pickett.** 2000. Transcriptional regulation of the antioxidant response element. Activation by Nrf2 and repression by MafK. J. Biol. Chem. 275:15466–15473.
34. **Pratico, D., and N. Delanty.** 2000. Oxidative injury in diseases of the central nervous system: focus on Alzheimer's disease. Am. J. Med. 109:577–585.
35. **Ramos-Gomez, M., M.-K. Kwak, P. M. Dolan, K. Itoh, M. Yamamoto, P. Talalay, and T. W. Kensler.** 2001. Sensitivity to carcinogenesis is increased and chemoprotective efficacy of enzymes inducers is lost in nrf2 transcription factor-deficient mice. Proc. Natl. Acad. Sci. USA 98:3410–3415.
36. **Reinheckel, T., N. Sitte, O. Ullrich, U. Kuckelkorn, K. J. Davies, and T. Grune.** 1998. Comparative resistance of the 20S and 26S proteasome to oxidative stress. Biochem. J. 335:637–642.
37. **Sekhar, K. R., S. R. Soltaninassab, M. J. Borrelli, Z. Q. Xu, M. J. Meredith, F. E. Domann, and M. L. Freeman.** 2000. Inhibition of the 26S proteasome induces expression of GLCLC, the catalytic subunit for gamma-glutamylcysteine synthetase. Biochem. Biophys. Res. Commun. 270:311–317.
38. **Shapiro, T. A., J. W. Fahey, K. L. Wade, K. K. Stephenson, and P. Talalay.** 2001. Chemoprotective glucosinolates and isothiocyanates of broccoli sprouts: metabolism and excretion in humans. Cancer Epidemiol. Biomarkers Prev. 10:501–508.
39. **Sherman, M. Y., and A. L. Goldberg.** 2001. Cellular defenses against unfolded proteins: a cell biologist thinks about neurodegenerative diseases. Neuron 29:15–32.
40. **Shringarpure, R., and K. J. Davies.** 2002. Protein turnover by the proteasome in aging and disease. Free Radic. Biol. Med. 32:1084–1089.
41. **Stephens, N. G., A. Parsons, P. M. Schofield, F. Kelly, K. Cheeseman, and M. J. Mitchinson.** 1996. Randomised controlled trial of vitamin E in patients with coronary disease: Cambridge Heart Antioxidant Study (CHAOS). Lancet 347:781–786.
42. **Takabe, W., T. Kodama, T. Hamakubo, K. Tanaka, T. Suzuki, H. Aburatani, N. Matsukawa, and N. Noguchi.** 2001. Anti-atherogenic antioxidants regulate the expression and function of proteasome alpha-type subunits in human endothelial cells. J. Biol. Chem. 276:40497–40501.
43. **Thimmulappa, R. K., K. H. Mai, S. Srisuma, T. W. Kensler, M. Yamamoto, and S. Biswal.** 2002. Identification of Nrf2-regulated genes induced by the chemopreventive agent sulforaphane by oligonucleotide microarray. Cancer Res. 62:5196–5203.
44. **Tiemann, F., and W. Deppert.** 1994. Immortalization of BALB/c mouse embryo fibroblasts alters SV40 large T-antigen interactions with the tumor

suppressor p53 and results in a reduced SV40 transformation-efficiency. Oncogene 9:1907–1915.

44a. **Wakabayashi, N., K. Itoh, J. Wakabayashi, H. Motohashi, S. Noda, S. Takahashi, S. Imakado, T. Kotsuji, F. Otsuka, D. R. Roop, T. Harada, J. D. Engel, and M. Yamamoto.** 28 September 2003. Keap-null mutation leads to postnatal lethality due to constitutive Nrf2 activation. Nat. Genet. 10.1038/ng1248.

45. **Wang, J. S., X. Shen, X. He, Y. R. Zhu, B. C. Zhang, J. B. Wang, G. S. Qian, S. Y. Kuang, A. Zarba, P. A. Egner, L. P. Jacobson, A. Munoz, K. J. Helzlsouer, J. D. Groopman, and T. W. Kensler.** 1999. Protective alterations in phase 1 and 2 metabolism of aflatoxin B1 by oltipraz in residents of Qidong, People's Republic of China. J. Natl. Cancer Inst. 91:347–354.

46. **Wasserman, W. W., and W. E. Fahl.** 1997. Functional antioxidant responsive elements. Proc. Natl. Acad. Sci. USA 94:5361–5366.

47. **Xie, Y., and A. Varshavsky.** 2001. RPN4 is a ligand, substrate, and transcriptional regulator of the 26S proteasome: a negative feedback circuit. Proc. Natl. Acad. Sci. USA 98:3056–3061.

48. **Yoo, J. Y., and S. Desiderio.** 2003. Innate and acquired immunity intersect in a global view of the acute-phase response. Proc. Natl. Acad. Sci. USA 100:1157–1162.

49. **Zhang, Y., P. Talalay, C. G. Cho, and G. H. Posner.** 1992. A major inducer of anticarcinogenic protective enzymes from broccoli: isolation and elucidation of structure. Proc. Natl. Acad. Sci. USA 89:2399–2403.

MOLECULAR AND CELLULAR BIOLOGY, Jan. 2004, p. 36–45 Vol. 24, No. 1
0270-7306/04/$08.00+0 DOI: 10.1128/MCB.24.1.36–45.2004

Transcription Factor Nrf2 Regulates Inflammation by Mediating the Effect of 15-Deoxy-$\Delta^{12,14}$-Prostaglandin J_2

Ken Itoh,[1,2]† Mie Mochizuki,[3]† Yukio Ishii,[3] Tetsuro Ishii,[4] Takahiro Shibata,[5] Yoshiyuki Kawamoto,[5] Vincent Kelly,[1,2] Kiyohisa Sekizawa,[3] Koji Uchida,[4] and Masayuki Yamamoto[1,2]*

ERATO Environmental Response Project,[1] Institute of Basic Medical Sciences and Center for Tsukuba Advanced Research Alliance,[2] Institute of Clinical Medicines,[3] and Institute of Social Medicines,[4] University of Tsukuba, Tsukuba 305-8577, and Laboratory of Food and Biodynamics, Graduate School of Bioagricultural Sciences, Nagoya University, Nagoya 464-8601,[5] Japan

Received 25 April 2003/Returned for modification 17 July 2003/Accepted 26 September 2003

Activated macrophages express high levels of Nrf2, a transcription factor that positively regulates the gene expression of antioxidant and detoxication enzymes. In this study, we examined how Nrf2 contributes to the anti-inflammatory process. As a model system of acute inflammation, we administered carrageenan to induce pleurisy and found that in Nrf2-deficient mice, tissue invasion by neutrophils persisted during inflammation and the recruitment of macrophages was delayed. Using an antibody against 15-deoxy-$\Delta^{12,14}$-prostaglandin J_2 (15d-PGJ_2), it was observed that macrophages from pleural lavage accumulate 15d-PGJ_2. We show that in mouse peritoneal macrophages 15d-PGJ_2 can activate Nrf2 by forming adducts with Keap1, resulting in an Nrf2-dependent induction of heme oxygenase 1 and peroxiredoxin I (PrxI) gene expression. Administration of the cyclooxygenase 2 inhibitor NS-398 to mice with carrageenan-induced pleurisy caused persistence of neutrophil recruitment and, in macrophages, attenuated the 15d-PGJ_2 accumulation and PrxI expression. Administration of 15d-PGJ_2 into the pleural space of NS-398-treated wild-type mice largely counteracted both the decrease in PrxI and persistence of neutrophil recruitment. In contrast, these changes did not occur in the Nrf2-deficient mice. These results demonstrate that Nrf2 regulates the inflammation process downstream of 15d-PGJ_2 by orchestrating the recruitment of inflammatory cells and regulating the gene expression within those cells.

When animals are exposed to environmental electrophiles, including xenobiotics, drugs, toxins, and carcinogens, even at nontoxic doses, the expression of a battery of genes that are essential to cellular defense mechanisms is induced. This process of gene induction is mediated by the antioxidant-responsive element (ARE) (31, 32). An increasing number of studies have identified genes regulated by ARE. These include genes encoding the phase II detoxication enzymes, such as glutathione *S*-transferase and quinone reductase, as well as antioxidative defense enzymes, such as heme oxygenase 1 (HO-1) and enzymes involved in glutathione synthesis (32). The cooperative activity of these enzymes serves to detoxify electrophiles and oxidative stress products.

Nrf2 is a member of the leucine zipper transcription factor family, and its activity is pivotal for the coordinate induction of phase II detoxifying and antioxidative enzymes whose expression is under the regulatory influence of ARE (15, 16, 18, 41). Nrf2 thus contributes to cytoprotection against environmental electrophiles and oxidative stresses (1, 4, 7, 11, 16, 33). Consistent with its assigned role in protection from environmental stress, Nrf2 is highly expressed in detoxication organs, including the gastrointestinal tract, liver, kidney, and lung. In addition, Nrf2 is abundantly expressed in activated macrophages, thyroid glands, and brown adipose tissue, suggesting additional physiological roles beyond detoxication (5).

The inflammatory response requires a coordinated integration of various signaling pathways, including cyclooxygenases (COX), nitric oxide, and cytokines (28, 40). COX enzymes catalyze the conversion of arachidonic acid to prostaglandin H_2 (PGH_2), from which other prostaglandins (PGs) are derived by the concomitant action of a variety of PG synthetases. Of the COX enzymes, COX-2 is found mainly in inflammatory cells and tissues. COX-2 is found to be upregulated during acute inflammation (37). By producing PGH_2, COX-2 promotes the synthesis of PGE_2, an important component of the inflammatory cascade that manifests many of the cardinal signs of inflammation (10). Intriguingly, since COX-2 is also expressed in the late phase of inflammation, it is widely accepted that COX-2 is associated with the resolution, as well as the establishment, of the acute inflammatory response (13). However, in contrast to the case during early stages of inflammation, pleural exudates of rats taken during the resolution stage of inflammation were found to contain high concentrations of PGD_2 and 15-deoxy-$\Delta^{12,14}$-PGJ_2 (15d-PGJ_2) with minimal levels of PGE_2 expression.

PGs can be divided into two subtypes: conventional PGs and cyclopentenone PGs (cyPGs) (44). Conventional PGs, such as PGE_2 and PGD_2, bind to cell surface receptors to exert their actions. However, no cell surface receptors have been identified for cyPGs, such as 15d-PGJ_2 and PGA_2. Rather, cyPGs are actively transported into cells, where they accumulate in nuclei and act as potent repressors of cell growth and inducers of cell

* Corresponding author. Mailing address: Center for TARA, University of Tsukuba, 1-1-1 Tennoudai, Tsukuba 305-8577, Japan. Phone: 81-298-53-6158. Fax: 81-298-53-7318. E-mail: masi@tara.tsukuba.ac.jp.

† K.I. and M.M. contributed equally to this work.

differentiation (12, 29). It has been reported that 15d-PGJ_2 exerts its anti-inflammatory activity through activation of peroxisome proliferator-activated receptor γ (PPARγ) (21, 34) or by directly inhibiting nuclear factor kappa B (NF-κB) activation by binding covalently to the IκB kinase (36).

Recently, Nrf2 target genes in macrophages were suspected of playing anti-inflammatory roles. For instance, HO-1 exerts anti-inflammatory functions in various systems, including carrageenan-induced pleurisy, through generation of carbon monoxide (30, 43). Furthermore, human peroxiredoxin I (PrxI or PAG) was recently identified as a negative regulator of macrophage migration inhibitory factor (MIF) (22), a crucial factor in the regulation of inflammation (26) and sepsis (35). These observations led us to explore possible roles for Nrf2 in the acute inflammatory response. To this end, we exploited carrageenan-induced pleurisy in mice as a model system. The results of this study reveal that the Nrf2-ARE system regulates the acute inflammation process by orchestrating the recruitment of inflammatory cells. We also found that COX-2 mediates the intracellular accumulation of 15d-PGJ_2 and that 15d-PGJ_2, which is shown to activate Nrf2, in turn regulates the expression of PrxI and other anti-oxidative stress enzymes in activated inflammatory macrophages.

MATERIALS AND METHODS

RNA blot hybridization analysis. Total cellular RNAs were extracted from macrophages by use of RNAzol (Tel-Test, Friendswood, Tex.). The RNA samples (10 μg) were electrophoresed and transferred to Zeta-Probe GT membranes (Bio-Rad). The membranes were probed with ^{32}P-labeled cDNA probes as indicated in the figures. β-Actin cDNA was used as a positive control.

RT-PCR analysis. Total RNAs (1 μg) were reverse transcribed into cDNA and used for a reverse transcription-PCR (RT-PCR) analysis (Qiagen, Hilden, Germany). GAPDH (glyceraldehyde-3-phosphate dehydrogenase) was used as a positive control. The PCR products were separated in a 1.5% agarose gel, and positive signals were quantified by densitometry analysis after staining with ethidium bromide.

Immunoblotting. The nuclei of peritoneal macrophages were solubilized with sodium dodecyl sulfate (SDS) sample buffer without loading dye and 2-mercaptoethanol, and protein concentrations were estimated by the bicinchoninic acid protein assay (Pierce, Rockford, Ill.). Proteins were separated by SDS-polyacrylamide gel electrophoresis in the presence of 2-mercaptoethanol and electrotransferred onto Immobilon membranes (Millipore). To detect immunoreactive proteins, we used horseradish peroxidase-conjugated anti-rabbit immunoglobulin G and ECL blotting reagents (Amersham). An anti-Nrf2 antibody was used as previously described (16). Inflammatory cell pellets from pulmonary lavage were lysed by sonication in buffer containing 50 mM Tris-HCl (pH 7.4), 25 mM KCl, 5 mM $MgCl_2$, 1 mM EDTA, 1% Nonidet P-40, and protease inhibitors. After centrifugation at 8,000 × *g* for 5 min at 4°C, protein concentrations in the supernatants were determined by the Bio-Rad protein assay. Samples were boiled with gel loading buffer (62.5 mM Tris-HCl, 2% SDS, 25% glycerol, and 0.01% bromophenol blue) at a ratio of 1:1 for 5 min. Total protein equivalents for each sample were separated by SDS–5 to 15% polyacrylamide gel electrophoresis in the presence of 2-mercaptoethanol and were transferred to Sequi-Blot polyvinylidene difluoride membranes (Bio-Rad). Blots were incubated with polyclonal rabbit antibody against murine PrxI (17).

Carrageenan-induced pleurisy. Wild-type and *nrf2*$^{-/-}$ mice of the ICR/129SV background weighing 20 to 25 g were used throughout the experiments. A 0.25% lambda carrageenan solution in saline (0.1 ml) was injected into the right pleural cavities of the animals. At 2, 6, 12, 24, 48, and 72 h and 7 days after the injection of carrageenan, the chest was carefully opened and the pleural cavity was washed with 1 ml of saline solution containing heparin. The pleural cavity was washed five times consecutively in the same way, and the pleural lavage fluid was collected into a tube.

Leukocyte counts. A 30-μl sample of collected pleural lavage fluid was diluted with Turk's solution, and total leukocytes were counted under an optical microscope. Differential leukocyte counts were determined in cytospin smears stained with Wright-Giemsa stain (Diff-Quick; Sysmex, Kobe, Japan).

TABLE 1. Number of neutrophils and albumin concentration in pleural lavage fluid

Time (h) and treatment	Neutrophils (10^4)[a]		Albumin (mg/ml)[a]	
	Nrf2$^{+/+}$ mice	Nrf2$^{-/-}$ mice	Nrf2$^{+/+}$ mice	Nrf2$^{-/-}$ mice
0	1 ± 0	1 ± 0	0.27 ± 0.07	0.30 ± 0.14
12				
Vehicle	179 ± 53[c]	128 ± 48	0.38 ± 0.14	0.26 ± 0.09
Carrageenan	492 ± 59[b,c]	508 ± 56[b,c]	0.68 ± 0.22[b,c]	0.87 ± 0.36[b,c]
24				
Vehicle	27 ± 18	21 ± 14	0.30 ± 0.18	0.31 ± 0.22
Carrageenan	229 ± 10[b,c]	386 ± 56[b,c]	1.1 ± 0.30[b,c]	1.5 ± 0.26[b,c]

[a] Data are means ± SEM. At least three mice were examined for each group.
[b] Significantly different from time-matched vehicle control mice ($P < 0.05$).
[c] Significantly different from genotype-matched 0-h control mice ($P < 0.05$).

Albumin concentration. The first washing was centrifuged at 400 × *g* for 5 min at 4°C, and the albumin concentration in the supernatant was determined with the albumin reagent from Sigma (St. Louis, Mo.).

Immunohistochemical analysis. Cells were smeared onto poly-L-lysine-coated slides and allowed to air dry. Endogenous peroxidases were quenched with 0.3% H_2O_2 in methanol, and sections were washed with 0.1% Triton X-100 in phosphate-buffered saline. The sections were reacted with anti-15d-PGJ_2 monoclonal antibody (38), anti-Prxl antibody (16), anti-HO-1 antibody (a generous gift from Shigeru Taketani), anti-F4/80 antibody (Serotec), anti-COX-2 antibody (Santa Cruz), or anti-hematopoietic PG synthetase (PGDS) antibody (Santa Cruz) and incubated for another hour with Histofine Simple Stain MAX-PO (Nichirei, Tokyo, Japan). Diaminobenzidine was used as a chromogen.

NS-398 and indomethacin treatment. NS-398 (Cayman Chemical, Ann Arbor, Mich.) (10 mg/kg) and indomethacin (Sigma) (10 mg/kg) were administered intraperitoneally 1 h before the injection of carrageenan. The pleural cavity was washed at 2, 12, and 24 h after the injection of carrageenan for the determination of inflammatory cell numbers and albumin concentration. To determine the effects of NS-398 at 48 and 72 h and 7 day, NS-398 was administered every 24 h thereafter. At 48 h, 72 h, and 7 days after the injection of carrageenan, the pleural cavity was washed for the determination of inflammatory cell numbers and albumin concentration.

15d-PGJ_2 administration. At 1 h after the intraperitoneal injection of NS-398, 15d-PGJ_2 (100 μg/kg) was injected into the pleural cavity. At 24 h after the injection of carrageenan, the pleural cavity was washed for the determination of inflammatory cell numbers and anti-inflammatory gene expression levels.

Statistical analysis. Statistical analysis was done by analysis of variance followed by a Bonferroni posttest. Albumin concentration data were analyzed by using Welch's *t* test. A *P* value of less than 0.05 was accepted as statistically significant.

RESULTS

Persistence of inflammatory cells in *nrf2*$^{-/-}$ mice during carrageenan-induced pleurisy. To explore the influence of Nrf2 during acute inflammation, we examined the effect of *nrf2* gene disruption on carrageenan-induced pleurisy in mice. In our preliminary experiments we administered 1% carrageenan to mice, a dose that is commonly used to induce carrageenan pleurisy in rodents, but we found that this particular dose provoked severe and protracted inflammation in mice as judged by neutrophil infiltration into the pleural cavity. We therefore carefully tested the correlation between the carrageenan dose and the duration of inflammation, finding that administration of 0.25% carrageenan reproduces the time course of acute inflammation and recovery (data not shown). Vehicle treatment caused a transient infiltration of neutrophils, which peaked at 12 h, but did not significantly alter the

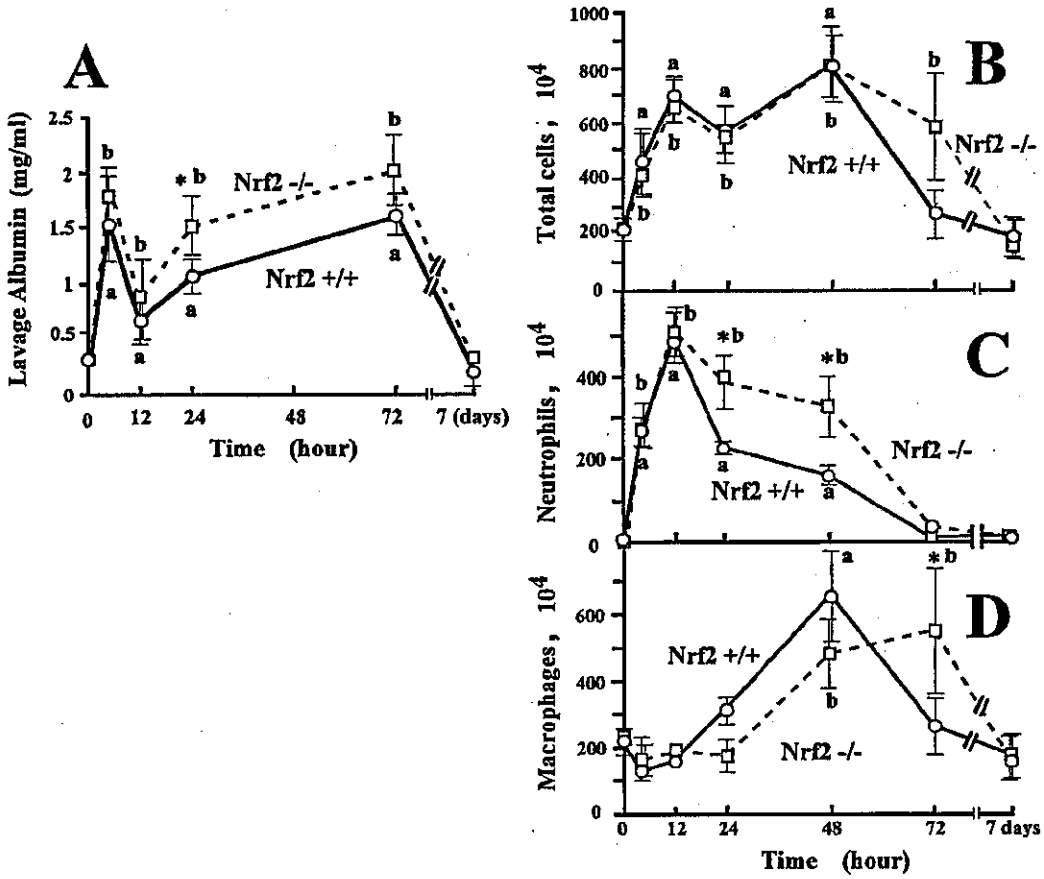

FIG. 1. Persistence of inflammatory cells in Nrf2-deficient mice in carrageenan-induced pleurisy. (A) Concentrations of pleural lavage albumin were measured at the indicated time points of pleurisy, and the means and standard deviations of triplicates are shown. (B to D) The numbers of total inflammatory cells (B), neutrophils (C), and macrophages (D) were counted microscopically at the indicted time points of pleurisy, and the means and standard deviations of triplicates are shown. Solid lines indicate the results for *nrf2*$^{+/+}$ mice, whereas dashed lines indicate the results for *nrf2*$^{-/-}$ mice. The means from four experiments are presented with standard errors of the mean. *, significantly different from time-matched wild-type mice ($P < 0.05$). a, significantly different from non-carrageenan-treated wild-type mice at the 0-h time point ($P < 0.05$). b, significantly different from non-carrageenan-treated *nrf2*$^{-/-}$ mice at the 0-h time point ($P < 0.05$).

albumin concentration (Table 1) and macrophage recruitment (data not shown) at the 12- and 24-h time points. In contrast, 0.25% carrageenan provoked a significant increase of neutrophil and albumin concentrations in the pleural lavage fluid (Table 1) compared to the vehicle-treated mice.

The albumin concentration in the pleural lavage fluid showed two peaks, one at 2 h and the other at 72 h after carrageenan injection, and then returned to normal levels by day 7 of pleurisy in both wild-type and *nrf2*$^{-/-}$ mice (Fig. 1A). The albumin concentration in pleural lavage fluid was significantly higher in *nrf2*$^{-/-}$ mice during pleurisy than in wild-type mice at the 24-h time point. The total inflammatory cell number in the pleural lavage fluid peaked at 12 and 48 h of pleurisy in both wild-type and *nrf2*$^{-/-}$ mice (Fig. 1B), but the infiltration of the cells persisted until 72 h of pleurisy in *nrf2*$^{-/-}$ mice. We speculated that an increase in neutrophils and macrophages at different time points might be responsible for the two peaks of infiltrated cells. We therefore examined the numbers of neutrophils (Fig. 1C) and macrophages (Fig. 1D) in the pleural lavage fluid. In wild-type mice, the neutrophil number peaked at 12 h and returned to the background level at 72 h of pleurisy, indicating that the first peak of total infiltrated cells mainly reflected an increase in neutrophils. Although in *nrf2*$^{-/-}$ mice, the magnitude of neutrophil infiltration was not significantly different from that in wild-type mice, the increased number of neutrophils persisted to later time points of pleurisy. The number of neutrophils in the pleural lavage fluid from *nrf2*$^{-/-}$ mice was significantly higher than that in wild-type mice at 24 and 48 h (Fig. 1C).

In contrast, macrophages were recruited to the pleural space at a later phase of pleurisy than the peak of neutrophil infiltration (Fig. 1D). The increase of macrophage number peaked at 48 h after the carrageenan administration and returned to the control level at the 72-h time point in wild-type mice, indicating that the second peak of total infiltrated cells mainly reflected an increase in macrophages. In contrast, macrophage recruitment peaked at the 72-h time point in *nrf2*$^{-/-}$ mice. The number of macrophages at this time point was significantly different from that in wild-type mice (Fig. 1D). Collectively, these results demonstrate that Nrf2 deficiency leads to a per-

sistence of neutrophil occupation and a delay of macrophage recruitment in carrageenan-induced pleurisy of mice.

15d-PGJ_2 accumulates in pleural inflammatory macrophages. Since 15d-PGJ_2 has been implicated as a key regulator of carrageenan pleurisy (8, 13, 44), we examined whether 15d-PGJ_2 accumulates in pleural inflammatory cells by using a specific monoclonal antibody against 15d-PGJ_2. The antibody has successfully detected the accumulation of 15d-PGJ_2 in both RAW264.7 cells activated by lipopolysaccharide and foamy macrophages of human atherosclerotic lesions (38). Furthermore, this antibody has shown to react almost exclusively with 15d-PGJ_2 (38). Immunohistochemical analysis with this antibody revealed that accumulation of 15d-PGJ_2 specifically occurred in pleural macrophages that were positive for F4/80 antigens but did not occur in neutrophils (data not shown).

As reported previously for rat carrageenan pleurisy, the accumulation of 15d-PGJ_2 showed two peaks (13). The accumulation of 15d-PGJ_2 was transiently observed at 2 h of pleurisy (Fig. 2A), but the accumulation then decreased at 6 h of pleurisy (Fig. 2B). At 2 h of pleurisy, the inducible accumulation of 15d-PGJ_2 in macrophages appeared to occur strongly around the nuclear membranes of resident pleural macrophages, which are small and round. The level increased again at 12 h after the carrageenan injection and remained high until 48 h of pleurisy (Fig. 2C and data not shown), followed by another increase at 72 h of pleurisy (Fig. 2D). At the 24-h time point, the accumulation of 15d-PGJ_2 was observed mainly in the cytoplasm of macrophages, which were large and had a foamy appearance (Fig. 2C). These results thus demonstrate that 15d-PGJ_2 specifically accumulates in pleural inflammatory macrophages and suggest that 15d-PGJ_2 may act through modifying macrophage function.

The Nrf2-Keap1 pathway mediates the induction of a range of genes by 15d-PGJ_2 in mouse peritoneal macrophages. cyPGs, including 15d-PGJ_2, have a reactive α,β-unsaturated carbonyl group in the cyclopentane ring. This ring structure renders this molecule capable of forming Michael adducts with nucleophilic cellular molecules and covalent modification of specific proteins. We speculate that this feature of cyPGs may activate Nrf2 (39). In order to obtain solid evidence for activation of the Nrf2 pathway by 15d-PGJ_2, we first examined the effect of exogenous 15d-PGJ_2 on the induction of three Nrf2 target genes in primary cultures of mouse peritoneal macrophages, which were used previously for the study of Nrf2 (16). The results clearly indicated that 15d-PGJ_2 activates, in a dose-dependent manner, the expression of the *HO-1*, *PrxI*, and *A170* genes (Fig. 3A), all of which were shown to be inducible by electrophiles in peritoneal macrophages (16).

We then examined which prostaglandins could strongly activate Nrf2 by using the peritoneal macrophage system. Of arachidonic acid and the arachidonic acid metabolites, including PGA_1, PGB_2, PGD_2, PGE_2, $PGF_{1\alpha}$, 15d-PGJ_2, thromboxane B_2, and leukotriene B_4, only PGA_1, 15d-PGJ_2, and PGD_2 markedly induced the expression of Nrf2 target genes (Fig. 3B). PGA_1 and 15d-PGJ_2 are classified as electrophilic cyPGs. Since PGD_2 is readily metabolized to 15d-PGJ_2 (38), 15d-PGJ_2 is suggested to be the most important cyPG in the regulation of Nrf2.

cyPGs activate Nrf2 in macrophages and hepatocytes. Subsequently, we examined the requirement for Nrf2 in the induction of antioxidant genes, using primary cultures of peritoneal macrophages from Nrf2-deficient mice. While HO-1, PrxI, and A170 mRNAs were all induced in wild-type macrophages by the addition of 5-μM 15d-PGJ_2 to the culture medium (Fig. 4A, lane 2), the induction was not observed in *nrf2*$^{-/-}$ macro-

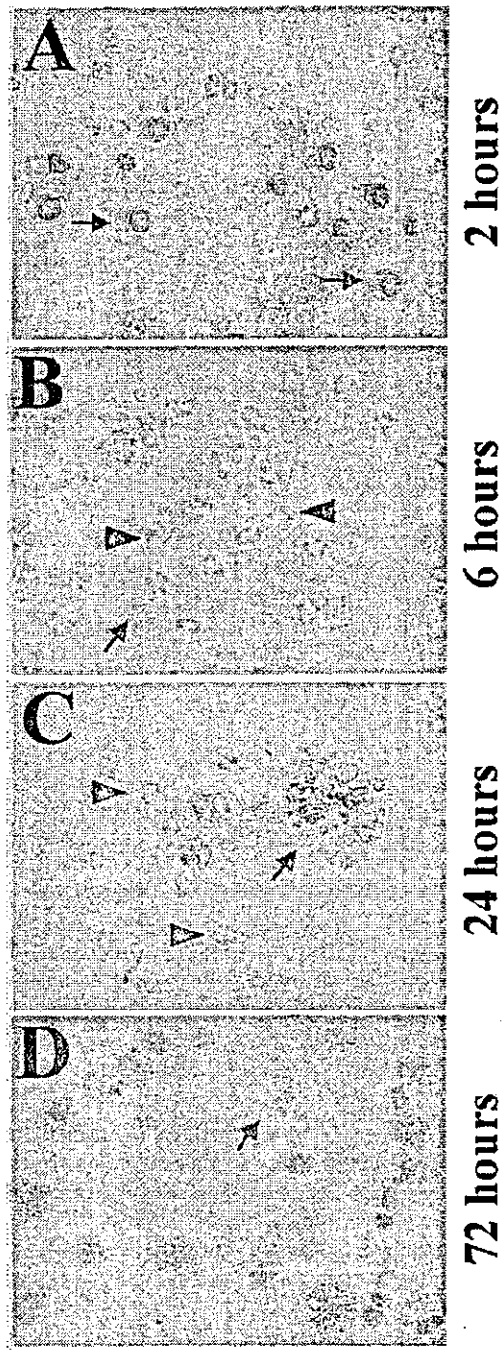

FIG. 2. Accumulation of 15d-PGJ_2 (brown) in pleural macrophages during carrageenan-induced pleurisy. Pleural inflammatory cells were examined immunohistochemically at the indicated times of pleurisy with anti-15d-PGJ_2 antibody. Arrows indicate macrophages, while arrowheads indicate neutrophils.

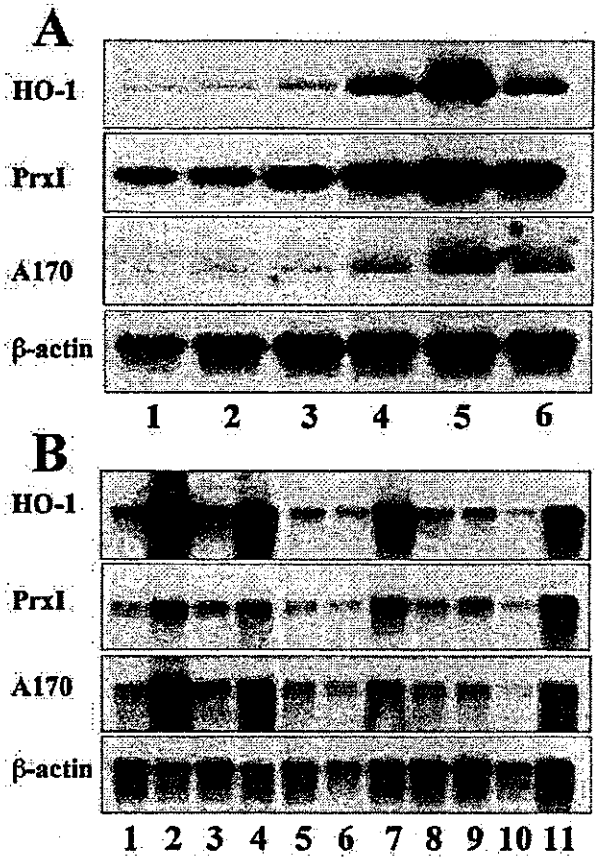

FIG. 3. cyPGs activate a set of antioxidant and anti-inflammatory genes in mouse peritoneal macrophages. (A) Peritoneal macrophages were treated with dimethyl sulfoxide alone (lane 1); with 15d-PGJ_2 at 0.5 μM (lane 2), 1 μM (lane 3), 5 μM (lane 4), or 10 μM (lane 5) for 5 h; or with 100 μM diethylmaleate for 5 h (lane 6), and total RNAs were analyzed by RNA blot analysis with HO-1, PrxI, and A170 cDNAs as probes. A β-actin cDNA probe was used for a loading control. (B) Peritoneal macrophages were treated with dimethyl sulfoxide alone (lane 1), PGA_1 (50 μM) (lane 2), PGB_2 (50 μM) (lane 3), PGD_2 (50 μM) (lane 4), PGE_2 (50 μM) (lane 5), $PGF_{1\alpha}$ (50 μM) (lane 6), 15d-PGJ_2 (10 μM) (lane 7), thromboxane B_2 (50 μM) (lane 8), leukotriene B_4 (1 μM) (lane 9), arachidonic acid (50 μM) (lane 10), or diethylmaleate (100 μM) (lane 11). Total RNA fractions were analyzed by RNA blot analysis as for panel A.

phages (lane 6). The result was reproducible with 10-μM 15d-PGJ_2 (lanes 3 and 7), but in this case a weak induction was observed in the *nrf2*$^{-/-}$ macrophages (lane 7), suggesting the presence of a minor complementary pathway to Nrf2. Consistent with these results, immunoblot analysis with anti-Nrf2 antibody revealed that 15d-PGJ_2 (Fig. 4B, lane 3) and PGA_1 (lane 4), but not PGE_2 (lane 5), induced the nuclear accumulation of Nrf2.

Immunocytochemical analysis of the rat hepatocyte cell line RL34, using the anti-Nrf2 antibody, further demonstrated that under normal culture conditions Nrf2 is retained by Keap1 in the cytoplasm (Fig. 4C). However, after the addition of 15d-PGJ_2, Nrf2 is liberated from Keap1 and translocates to and accumulates within the nucleus (Fig. 4D).

Recent studies indicate that certain Nrf2 inducers, such as Michael reaction acceptors, directly bind to reactive cysteine residues in Keap1, thereby liberating Nrf2 (9). To elucidate whether 15d-PGJ_2 binds directly to Keap1, we examined the binding of biotin-tagged 15d-PGJ_2 to Keap1 in RL34 cells. A pull-down analysis with avidin beads followed by probing with anti-Keap1 antibody demonstrated that Keap1 could be detected in precipitates from biotinylated 15d-PGJ_2-treated or biotinylated Δ^{12}-PGJ_2-treated cells but not in the control immunoprecipitates (Fig. 4E). This result suggests that 15d-PGJ_2 directly binds to Keap1, most probably through covalent linkage, allowing Nrf2 to be released from Keap1.

COX-2 inhibitor affects the inflammatory cell infiltration. In order to elucidate the relationship between the accumulation of 15d-PGJ_2 and activation of Nrf2, we examined the time course of PrxI gene expression during the carrageenan-induced pleurisy. Immunoblot analyses with anti-PrxI antibody revealed that the expression of PrxI was induced at as early as 2 h of pleurisy (Fig. 5A, lanes 3 to 5). In contrast, the induction of PrxI during pleurisy was largely abolished in *nrf2*$^{-/-}$ mice, and this difference was prominent at 2 to 24 h (lanes 4, 7, and 10) but became relatively small after 48 h of pleurisy (lanes 13 and 16).

COX-2 is known to regulate PG synthesis in carrageenan pleurisy. To examine the role of COX-2 in the inducible expression of PrxI, we examined the in vivo effect of NS-398, a specific inhibitor of COX-2 (42), on PrxI expression. Peritoneal injection of NS-398 1 h before carrageenan treatment significantly attenuated the expression of PrxI in macrophages when tested by immunoblotting (Fig. 5A) and of 15d-PGJ_2 when tested by immunocytochemistry (data not shown). NS-398 caused a reduction of PrxI expression especially at 2 to 24 h (Fig. 5A, lanes 5, 8, and 11), but the effect was not as prominent after 48 h of pleurisy (lanes 14 and 17). These results suggest a possible scenario in which COX-2 mediates the accumulation of 15d-PGJ_2 and 15d-PGJ_2 in turn activates Nrf2 and regulates the expression of PrxI as well as the other antioxidant genes.

Immunohistochemical analysis demonstrated that PrxI expression was specifically observed in macrophages, but not in neutrophils, of pleural lavage fluid (Fig. 5B). The expression profile of PrxI clearly overlapped with those of 15d-PGJ_2 and macrophage-specific F4/80 antigen (Fig. 5B). The expression of HO-1 was also detected exclusively in pleural macrophages (Fig. 5B), in very good agreement with previous analysis of the rat pleurisy model. Furthermore, COX-2 and hematopoietic PGDS, two major rate-limiting enzymes for 15d-PGJ_2 synthesis, were highly expressed in the macrophages (Fig. 5B), supporting our contention that 15d-PGJ_2 was synthesized mainly in the macrophages.

It should be noted that NS-398 treatment caused a persistence of neutrophil infiltration at 24 h of pleurisy (Fig. 5C) and a delay in macrophage recruitment (Fig. 5D) in pleural lavage fluid. This is in contrast to the case for untreated mice, where the macrophage number was high at 48 h and decreased at 72 h of pleurisy. It can be observed that in the NS-398-treated mice the macrophage number continued to climb even at 72 h of pleurisy (Fig. 5D). Also, in the NS-398-treated mice, the macrophage number was rather low at the 24- and 48-h time points, indicating a delay in macrophage recruitment. The persistence of neutrophil infiltration and the delay of macrophage

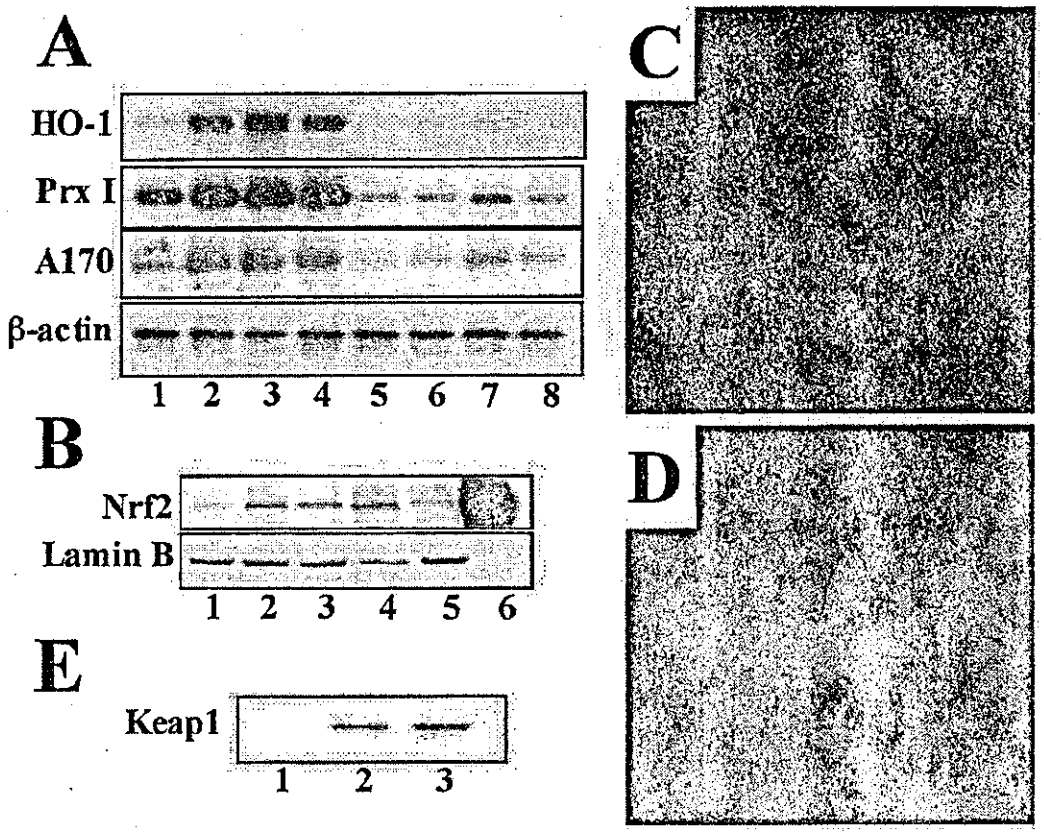

FIG. 4. cyPGs activate Nrf2 in macrophages and hepatocytes. (A) Peritoneal macrophages derived from either wild-type mice (lanes 1 to 4) or *nrf2*$^{-/-}$ mice (lanes 5 to 8) were treated with 5 μM (lanes 2 and 6) or 10 μM (lanes 3 and 7) 15d-PGJ_2 or with 100 μM diethylmaleate (lanes 4 and 8). Untreated controls are shown in lanes 1 and 5. Total RNAs were analyzed by RNA blotting analysis, using cDNAs for HO-1, PrxI, or A170 as probes. A β-actin cDNA probe was used for a loading control. (B) Nuclear extracts were prepared from macrophages untreated (lane 1) or treated with diethylmaleate (100 μM) (lane 2), 15d-PGJ_2 (5 μM) (lane 3), PGA_1 (100 μM) (lane 4), or PGE_2 (100 μM) (lane 5). The extracts were immunoblotted with anti-Nrf2 antibody or anti-lamin B antibody. Recombinant Nrf2 in 293T cells was also loaded as a control (lane 6). (C and D) RL34 cells were either untreated (C) or treated with 10 μM 15d-PGJ_2 for 4 h (D), and expression of Nrf2 were examined immunocytochemically with the anti-Nrf2 antibody. Subcellular localization of Nrf2 was analyzed by confocal microscopy. (E) RL34 cells were treated with dimethyl sulfoxide (lane 1), biotinylated Δ^{12}-PGJ_2 (lane 2), or biotinylated 15d-PGJ_2 (lane 3). Keap1-PGJ_2 complexes were precipitated from the cell extracts with avidin beads and probed with the anti-Keap1 antibody.

recruitment were also observed in the COX-1/COX-2 dual inhibitor indomethacin (Fig. 5E). Thus, inflammatory cell infiltration in COX-2-inhibited mice closely reflects that observed in Nrf2-deficient mice, further supporting our contention that 15d-PGJ_2 (and COX-2) acts as a regulator of the Nrf2 pathway and the expression of antioxidant genes.

Replacement of 15d-PGJ_2 into the intrapleural space. Finally, we wished to test directly the significance of 15d-PGJ_2 accumulation in the development of and recovery from carrageenan-induced pleurisy. To this end, we administered 15d-PGJ_2 into the intrapleural cavity and examined changes in inflammatory cell infiltration at 24 h of pleurisy. Consistent with the results shown above, administration of NS-398 to mice with pleurisy increased the neutrophil number at 24 h (Fig. 6A, bar 2). We found that simultaneous injection of 15d-PGJ_2 with carrageenan into the pleural space reversed the increase of neutrophil infiltration in NS-398-treated mice (bar 3). The important finding here is that the administration of 15d-PGJ_2 into the pleural space of Nrf2-null mice did not affect the accumulation of neutrophils (compare bars 4 and 5).

We found the opposite result for macrophages recruitment during pleurisy. While the NS-398 treatment provoked a delay in the macrophage recruitment (Fig. 6B, bar 2), this was reversed by the simultaneous administration of 15d-PGJ_2 (bar 3). Nrf2 must therefore mediate this effect of 15d-PGJ_2, as 15d-PGJ_2 did not help to reverse the delay in macrophage recruitment in the Nrf2-deficient mice (compare bars 4 and 5).

To determine changes in the antioxidant gene expression, we carried out RT-PCR analyses with pleural inflammatory cells and specific primers for PrxI (Fig. 6C) and HO-1 (Fig. 6D). The expression of PrxI and HO-1 showed a pattern of changes similar to that for macrophage number. The NS-398-treatment produced a decrease in *PrxI* and *HO-1* gene expression (bar 2). On the other hand, the administration of 15d-PGJ_2 to the NS-398-treated mice reversed the PrxI and HO-1 mRNA expression level (bar 3) to that for wild-type control mice (bar 1). The expression levels of PrxI and HO-1 mRNAs in the Nrf2-deficient mice did not change with 15d-PGJ_2 treatment (compare bars 4 and 5). These results thus argue that 15d-PGJ_2 transduces the inflammatory signals to Nrf2 and that Nrf2

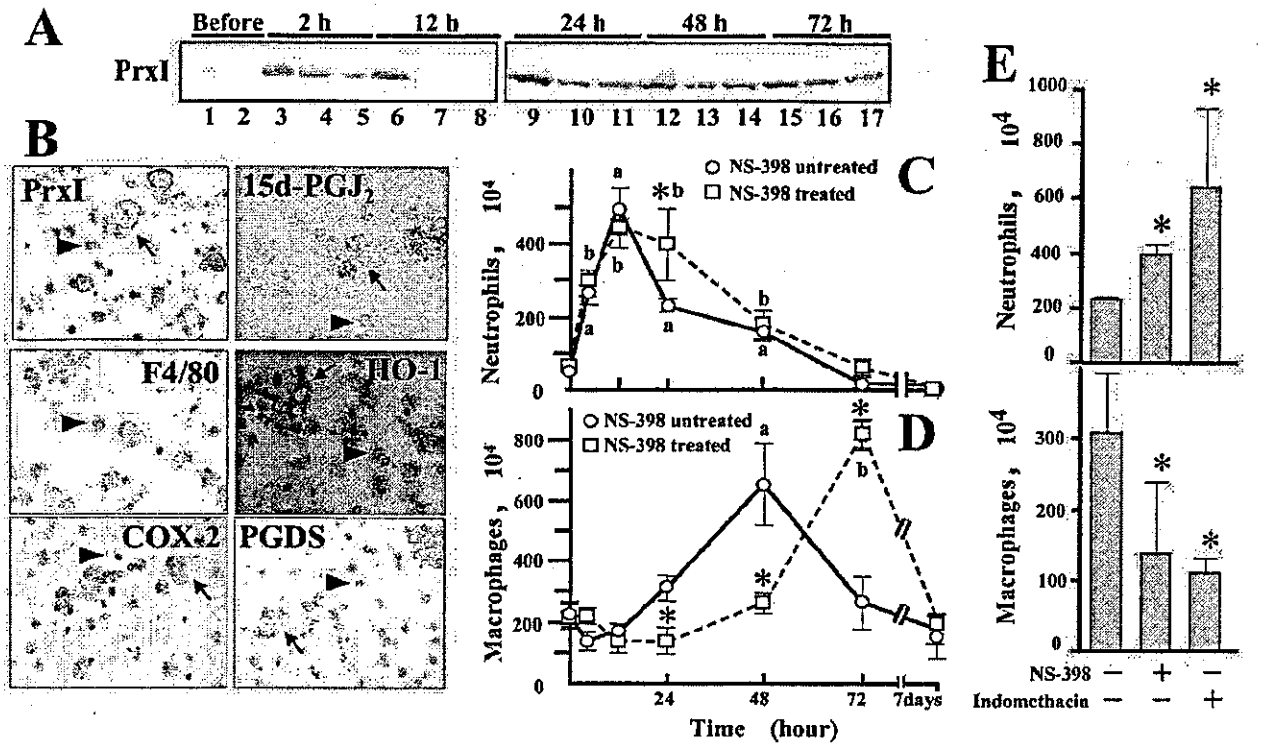

FIG. 5. PrxI expression at the early phase of carrageenan-induced pleurisy depends on both 15d-PGJ_2 and Nrf2. (A) Both the COX-2 inhibitor NS-398 and *nrf2* gene disruption affect PrxI expression during carrageenan-induced pleurisy. Whole-cell extracts of pleural inflammatory cells from wild-type mice (lanes 1, 3, 6, 9, 12, and 15), $nrf2^{-/-}$ mice (lanes 2, 4, 7, 10, 13, and 16), or NS-398-treated wild-type mice (lanes 5, 8, 11, 14, and 17) at the indicated time points of pleurisy were examined by immunoblotting with anti-PrxI antibody. (B) The expression of PrxI, 15d-PGJ_2, F4/80, HO-1, COX-2, and hematopoietic PGDS in pleural inflammatory cells at 24 h of pleurisy was analyzed immunohistochemically with the corresponding antibodies as indicated. Arrows indicate macrophages, while arrowheads represent neutrophils. (C and D) Administration of NS-398 affects neutrophil (C) and macrophage (D) numbers during carrageenan-induced pleurisy. The number of pleural inflammatory cells was microscopically counted, and the means from four experiments are presented with standard errors of the mean. *, significantly different from time-matched NS398-untreated mice ($P < 0.05$). a, significantly different from carrageenan-untreated wild-type mice at the 0-h time point ($P < 0.05$). b, significantly different from carrageenan-untreated $nrf2^{-/-}$ mice at the 0-h time point ($P < 0.05$). (E) Effect of indomethacin on pleural inflammatory cells. Cell counts were taken at 24 h of pleurisy. The means from four experiments are presented with standard errors of the mean. *, significantly different from untreated control mice ($P < 0.05$).

transcriptionally regulates both the antioxidant gene expression in pleural macrophages and inflammatory cell recruitment.

DISCUSSION

The cyPG 15d-PGJ_2 is emerging as a probable regulator of acute inflammation (13, 43–45). By exploiting carrageenan-induced pleurisy as a model system for acute inflammation, this study examined the relationship between 15d-PGJ_2 and Nrf2. We found that during carrageenan-induced pleurisy, 15d-PGJ_2 accumulates in pleural inflammatory cells and the accumulation is confined to macrophages. The results of this study unveil a number of significant correlations between accumulation of 15d-PGJ_2 and activation of Nrf2 during carrageenan-induced pleurisy. First, in Nrf2-deficient mutant mice, the accumulation of neutrophils during inflammation persisted and macrophage recruitment was delayed to the late phases of pleurisy. Second, the COX-2 inhibitor NS-398 and the COX-1/COX-2 dual inhibitor indomethacin, which attenuate the accumulation of 15d-PGJ_2, affected the acute inflammatory response in a manner similar to a deficiency in Nrf2. NS-398 repressed the expression of PrxI in pleural macrophages and caused a persistence of neutrophil accumulation with a concomitant delay in macrophage recruitment. Third, the administration of 15d-PGJ_2 into the pleural space reversed both the decrease of PrxI expression and persistence of neutrophils in NS-398-treated mice, whereas this treatment did not reverse a similar phenotype in the Nrf2-deficient mice, arguing strongly that 15d-PGJ_2 functions to activate Nrf2. Fourth, our data show that in peritoneal macrophages and hepatocytes, 15d-PGJ_2 directly bound to Keap1 and thereby liberated Nrf2. Taken together, these results demonstrate that Nrf2 regulates the acute inflammatory response by orchestrating the recruitment of inflammatory cells and regulating the expression of anti-oxidative stress genes downstream of 15d-PGJ_2.

Increasing lines of evidence (8, 44, 45) suggest that in addition to establishing acute inflammation, COX-2 also contributes to the resolution phase of inflammation through 15d-PGJ_2. 15d-PGJ_2 can function as both an activator and a repressor of signal-transducing transcription factors. The possible contributions made by 15d-PGJ_2 to the acute inflammatory response are summarized in Fig. 7. It has been reported

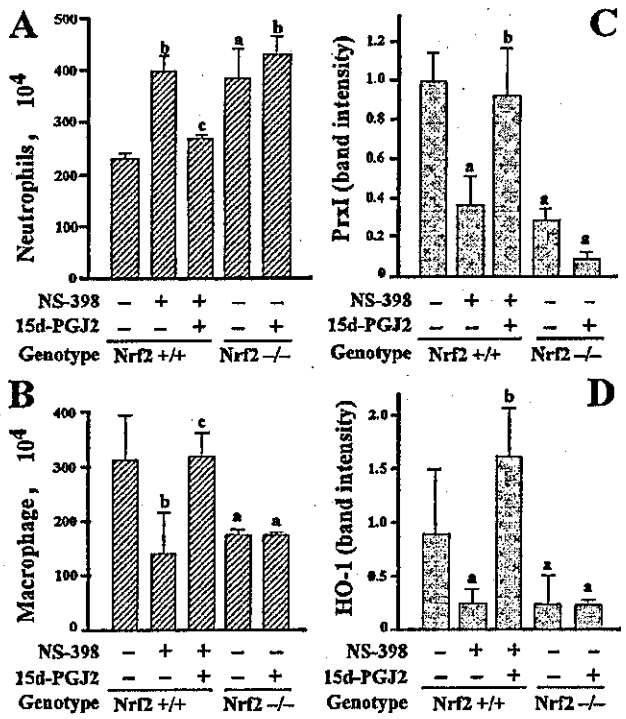

FIG. 6. Intrapleural injection of 15d-PGJ_2 reverses the decrease of PrxI expression and persistence of neutrophils in NS-398-treated mice but not in Nrf2-deficient mice. (A and B) Numbers of neutrophils (A) and macrophages (B) at 24 h of pleurisy in wild-type ($nrf2^{+/+}$) mice (bars 1), NS-398-treated $nrf2^{+/+}$ mice (bars 2), NS-398-treated $nrf2^{+/+}$ mice administrated 15d-PGJ_2 (bars 3), $nrf2^{-/-}$ mice (bars 4), and $nrf2^{-/-}$ mice administrated NS-398 (bars 5). Neutrophils and macrophages were counted microscopically, and the means and standard deviations of triplicates are shown. a, $P < 0.05$ compared with untreated control mice; b, $P < 0.01$ compared with untreated control mice; c, $P < 0.01$ compared with NS-398-treated wild-type mice. (C, D) RT-PCR analysis of PrxI (C) and HO-1 (D) mRNAs in pleural inflammatory cells in mice. Intensities of RT-PCR bands were quantified by densitometric analysis, and the means of triplicates are presented. a, $P < 0.01$ compared with untreated control group; b, $P < 0.01$ compared with NS-398-treated wild-type mice.

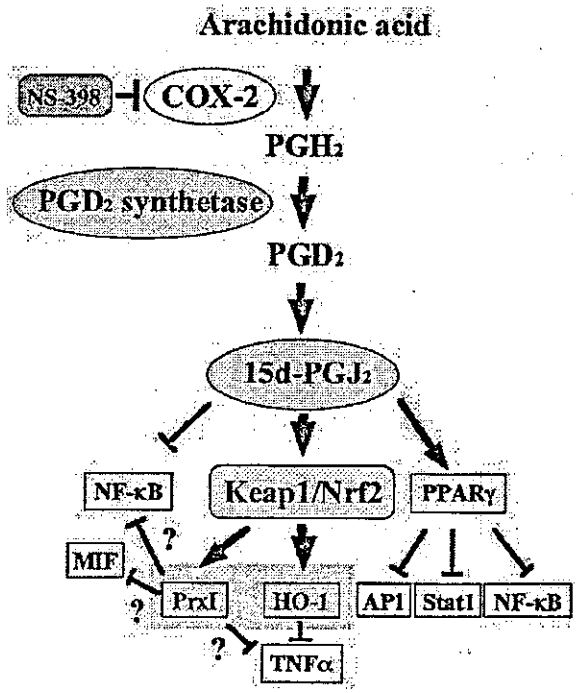

FIG. 7. Network of 15d-PGJ_2 and the Nrf2-Keap1 pathway in carrageenan-induced pleurisy. 15d-PGJ_2 is generated in pleural macrophages during carrageenan-induced pleurisy and is known to directly inhibit NF-κB activity and also to act as a ligand for PPARγ. This study shows that 15d-PGJ_2 activates the Nrf2-Keap1 pathway through covalent binding to Keap1. Nrf2 induces HO-1 and PrxI expression as well as other ARE-regulated genes in macrophages (green). The upregulation of PrxI appears to inhibit NF-κB, TNF-α, and the β-tautomerase activity of MIF, thus modulating the inflammation process. On the other hand, HO-1 is known to inhibit the expression of TNF-α through CO production.

that 15d-PGJ_2 inhibits NF-κB activation by covalently binding to IκB kinase β or the p50 subunit of NF-κB (3, 36). In addition, 15d-PGJ_2 has been reported to serve as a natural ligand of PPARγ (21, 34). Activated PPARγ regulates the synthesis of proinflammatory cytokines and the induction of nitric oxide synthetase in activated monocytes by negatively interacting with AP-1, NF-κB, or STAT. Thus, 15d-PGJ_2 may have an impact upon multiple mechanisms during the resolution of inflammation. The results of this study demonstrate that 15d-PGJ_2 can act as a potent anti-inflammatory agent by exploiting the Nrf2-Keap1 pathway, a previously unrecognized alternative pathway in the cascades downstream of 15d-PGJ_2.

The possible involvement of Nrf2 in inflammation has been alluded to in some earlier reports. For instance, antirheumatic gold(I) compounds markedly activate Nrf2 (24). We found that female Nrf2 knockout mice frequently developed severe glomerulonephritis (46). Braun et al. recently reported that Nrf2 regulates inflammation during healing of skin wounds (2). The expression of several inflammatory cytokines was shown to persist during the healing of a skin wound in Nrf2-deficient mice, such that interleukin-1β levels in the wound remained elevated to day 13, most likely due to the persistence of macrophages at the site of the wound. Finally, ARE battery genes are activated by laminar shear stress, which acts as an anti-inflammatory signal in endothelial cells (6). Indeed, in endothelial cells, overexpression of Nrf2 inhibited the tumor necrosis factor alpha (TNF-α)-mediated induction of vascular cell adhesion molecule-1 gene expression, which is important for monocyte recruitment during inflammation response. Our present observations, along with those cited above, suggest that Nrf2 is important for regulating the process of acute inflammation.

We demonstrated in this study that the intracellular accumulation of 15d-PGJ_2 occurs during carrageenan-induced pleurisy in the mouse (Fig. 2). This observation is consistent with the previous analysis in rat carrageenan pleurisy, where 15d-PGJ_2 accumulates with two peaks at low nanomolar levels in the pleural exudates. As the 15d-PGJ_2 concentration used in this study is higher than that detected in pleural exudates, it might be challenging to hypothesize that 15d-PGJ_2 works as an endogenous regulator of acute inflammation. However, Narumiya et al. previously reported that exogenously added Δ^{12}-

PGJ_2 accumulates in the cells in a protein-bound form and is resistant to cell extraction, suggesting that intracellular sequestration of these cyPGs is most probably due to the Michael adduction to the protein (27). Furthermore, Keap1 localizes in the perinuclear cytoskeleton close to COX-2 and PGDS. Therefore, it is likely that the local concentration of cyPGs accumulates to a level sufficient for Nrf2 activation during pleurisy.

It was reported recently that submicromolar concentrations of 15d-PGJ_2 can activate HO-1 and contribute to the anti-inflammatory effect of this reagent (25). As NF-κB inhibition requires a concentration of 15d-PGJ_2 in the micromolar range in cell culture (36), this observation suggests that an in vivo anti-inflammatory effect of 15d-PGJ_2 may be more relevant to the activation of Nrf2.

Under normal conditions, Nrf2 activity is suppressed primarily by its compartmentalization to the cytosol by Keap1 and consequent rapid degradation by the proteasome (reference 20 and references therein). Recently it was demonstrated that electrophiles classified as Michael reaction acceptors directly bound to Keap1 and dissociated Nrf2 from Keap1 (9). We have demonstrated in this study that 15d-PGJ_2 and Δ^{12}-PGJ_2, both of which contain a reactive α,β-unsaturated carbonyl group in their cyclopentane ring, directly bind to Keap1 and activate Nrf2. These results are consistent with our contention that cyPGs act as endogenous activators of the Nrf2-Keap1 pathway in macrophages, thereby regulating the recruitment of inflammatory cells.

NS-398-treated wild-type mice and *nrf2*-null mice displayed similar phenotypes in pleurisy, i.e., a persistence of neutrophil residence and a delay in macrophage recruitment. These results suggest that COX-2 products negatively regulate the accumulation of neutrophils in the intrapleural space, through either enhancing the phagocytosis of neutrophils by macrophages or decreasing the neutrophil infiltration. The administration of 15d-PGJ_2 into the pleural space successfully reversed the phenotype in NS-398-treated mice, indicating that 15d-PGJ_2 works downstream of COX-2 activation. Consistent with this observation, we demonstrated in this study that the actual inducible accumulation of 15d-PGJ_2 occurred in macrophages during carrageenan pleurisy (Fig. 2). Since the introduction of 15d-PGJ_2 into the pleural spaces of Nrf2-deficient mice had no effect, Nrf2 must be a downstream mediator of 15d-PGJ_2 activity in macrophages. Thus, we conclude that 15d-PGJ_2 regulates acute inflammation through regulating the function of macrophages (Fig. 7).

It remains to be elucidated to how Nrf2 regulates acute inflammation. We speculate that a battery of Nrf2 target genes cooperatively function to repress proinflammatory signals, such as those of TNF-α or interleukin-1β. HO-1 and PrxI are the Nrf2 target genes that are likely to influence the inflammatory process (Fig. 7) (16). Recently, Gong et al. have demonstrated that 15d-PGJ_2 can activate HO-1 via a stress-responsive element and by an Nrf2-mediated mechanism (14). In the carrageenan-induced pleurisy model, it has been shown that elevation of HO-1 expression can suppress, whereas inhibition of HO-1 activity can exacerbate, the inflammatory response (43, 45). Indeed, HO-1 can inhibit the expression of TNF-α most probably through the generation of carbon monoxide (30). With respect to PrxI, its human counterpart PAG was reported to directly bind to and negatively regulate β-tautomerase activity of MIF, which is one of the central regulators of inflammation (22). Although the physiological significance of the β-tautomerase activity of MIF is unclear at present, we nonetheless expect that the repression of MIF activity by PrxI may play important roles in the regulation of inflammation. Furthermore, the overexpression of PrxI removed H_2O_2 (23), suggesting that PrxI can repress TNF-α signaling by the removal of H_2O_2 (Fig. 7). These observations suggest that Nrf2 may have multiple downstream targets that regulate the acute inflammation process.

In the rat carrageenan-induced pleurisy model, accumulation of 15d-PGJ_2 in the late phase of pleurisy was associated with resolution of the inflammation (13). However, the true role of 15d-PGJ_2 during the early phase of pleurisy remained largely unknown. Our results imply that in the early phase, accumulation of 15d-PGJ_2 activates Nrf2 and regulates the inflammation process through the induction of target gene expression, including that of HO-1 and PrxI. Whereas COX-2 has been reported to accelerate inflammation in the early phase of pleurisy through the induction of PGE_2, our present analyses suggest that COX-2 also can suppress the early phase of inflammation through the production of 15d-PGJ_2. These results are consistent with the present model that the inflammation process is balanced by an acceleration and deceleration of integrating signaling pathways (28). Understanding of how the signals are integrated to establish and resolve the acute inflammation process provides important clues to facilitate the development of effective treatments for chronic inflammation.

ACKNOWLEDGMENTS

We thank S. Taketani for providing the polyclonal antibody against rat HO-1. We also thank Y. Katoh, A. Kobayashi, M. Kobayashi, S. Nishimura, K. I. Tong, and N. Wakabayashi for discussion and advice.

This work was supported in part by grants from JST-ERATO; the Ministry of Education, Culture, Sports, Science and Technology; the Ministry of Health, Labor and Welfare; and the Naito foundation.

REFERENCES

1. **Aoki, Y., H. Sato, N. Nishimura, S. Takahashi, K. Itoh, and M. Yamamoto.** 2001. Accelerated DNA adduct formation in the lung of the Nrf2 knockout mouse exposed to diesel exhaust. Toxicol. Appl. Pharmacol. 173:154–160.
2. **Braun, S., C. Hanselmann, M. G. Gassmann, U. auf dem Keller, C. Born-Berclaz, K. Chan, Y. W. Kan, and S. Werner.** 2002. Nrf2 transcription factor, a novel target of keratinocyte growth factor action which regulates gene expression and inflammation in the healing skin wound. Mol. Cell. Biol. 22:5492–5505.
3. **Cernuda-Morollon, E., E. Pineda-Molina, F. J. Canada, and D. Perez-Sala.** 2001. 15-Deoxy-$\Delta^{12,14}$-prostaglandin J_2 inhibition of NF-κB-DNA binding through covalent modification of the p50 subunit. J. Biol. Chem. 276:35530–35536.
4. **Chan, K., and Y. W. Kan.** 1999. Nrf2 is essential for protection against acute pulmonary injury in mice. Proc. Natl. Acad. Sci. USA 96:12731–12736.
5. **Chan, K., R. Lu, J. C. Chang, and Y. W. Kan.** 1996. NRF2, a member of the NFE2 family of transcription factors, is not essential for murine erythropoiesis, growth, and development. Proc. Natl. Acad. Sci. USA 93:13943–13948.
6. **Chen, X. L., S. E. Varner, A. S. Rao, J. Y. Grey, S. Thomas, C. K. Cook, M. A. Wasserman, R. M. Medford, A. K. Jaiswal, and C. Kunsch.** 2003. Laminar flow induction of antioxidant response element-mediated genes in endothelial cells. A novel anti-inflammatory mechanism. J. Biol. Chem. 278:703–711.
7. **Cho, H. Y., A. E. Jedlicka, S. P. Reddy, T. W. Kensler, M. Yamamoto, L. Y. Zhang, and S. R. Kleeberger.** 2002. Role of NRF2 in protection against hyperoxic lung injury in mice. Am. J. Respir. Cell. Mol. Biol. 26:175–182.
8. **Cuzzocrea, S., N. S. Wayman, E. Mazzon, L. Dugo, R. Di Paola, I. Serraino, D. Britti, P. K. Chatterjee, A. P. Caputi, and C. Thiemermann.** 2002. The cyclopentenone prostaglandin 15-deoxy-$\Delta^{12,14}$-prostaglandin J_2 attenuates the development of acute and chronic inflammation. Mol. Pharmacol. 61: 997–1007.
9. **Dinkova-Kostova, A. T., W. D. Holtzclaw, R. N. Cole, K. Itoh, N. Wakaba-**

yashi, Y. Katoh, M. Yamamoto, and P. Talalay. 2002. Direct evidence that sulfhydryl groups of Keap1 are the sensors regulating induction of phase 2 enzymes that protect against carcinogens and oxidants. Proc. Natl. Acad. Sci. USA 99:11908–11913.
10. Di Rosa, M., J. P. Giroud, and D. A. Willoughby. 1971. Studies on the mediators of the acute inflammatory response induced in rats in different sites by carrageenan and turpentine. J. Pathol. 104:15–29.
11. Enomoto, A., K. Itoh, E. Nagayoshi, J. Haruta, T. Kimura, T. O'Connor, T. Harada, and M. Yamamoto. 2001. High sensitivity of Nrf2 knockout mice to acetaminophen hepatotoxicity associated with decreased expression of ARE-regulated drug metabolizing enzymes and antioxidant genes. Toxicol. Sci. 59:169–177.
12. Fukushima, M. 1992. Biological activities and mechanisms of action of PGJ2 and related compounds: an update. Prostaglandins Leukot. Essential Fatty Acids 47:1–12.
13. Gilroy, D. W., P. R. Colville-Nash, D. Willis, J. Chivers, M. J. Paul-Clark, and D. A. Willoughby. 1999. Inducible cyclooxygenase may have anti-inflammatory properties. Nat. Med. 5:698–701.
14. Gong, P., D. Stewart, B. Hu, N. Li, J. Cook, A. Nel, and J. Alam. 2002. Activation of the mouse heme oxygenase-1 gene by 15-deoxy-$\Delta^{12,14}$-prostaglandin J_2 is mediated by the stress response elements and transcription factor Nrf2. Antioxid. Redox Signal. 4:249–257.
15. Ishii, T., K. Itoh, and M. Yamamoto. 2002. Roles of Nrf2 in activation of antioxidant enzyme genes via antioxidant responsive elements. Methods Enzymol. 348:182–190.
16. Ishii, T., K. Itoh, S. Takahashi, H. Sato, T. Yanagawa, Y. Katoh, S. Bannai, and M. Yamamoto. 2000. Transcription factor Nrf2 coordinately regulates a group of oxidative stress-inducible genes in macrophages. J. Biol. Chem. 275:16023–16029.
17. Ishii, T., M. Yamada, H. Sato, M. Matsue, S. Taketani, K. Nakayama, Y. Sugita, and S. Bannai. 1993. Cloning and characterization of a 23-kDa stress-induced mouse peritoneal macrophage protein. J. Biol. Chem. 268: 18633–18636.
18. Itoh, K., T. Chiba, S. Takahashi, T. Ishii, K. Igarashi, Y. Katoh, T. Oyake, N. Hayashi, K. Satoh, I. Hatayama, M. Yamamoto, and Y. Nabeshima. 1997. An Nrf2/small Maf heterodimer mediates the induction of phase II detoxifying enzyme genes through antioxidant response elements. Biochem. Biophys. Res. Commun. 236:313–322.
19. Itoh, K., N. Wakabayashi, Y. Katoh, T. Ishii, K. Igarashi, J. D. Engel, and M. Yamamoto. 1999. Keap1 represses nuclear activation of antioxidant responsive elements by Nrf2 through binding to the amino-terminal Neh2 domain. Genes Dev. 13:76–86.
20. Itoh, K., N. Wakabayashi, Y. Katoh, T. Ishii, T. O'Connor, and M. Yamamoto. 2003. Keap1 regulates both cytoplasmic-nuclear shuttling and degradation of Nrf2 in response to electrophiles. Genes Cells 8:379–381.
21. Jiang, C., A. T. Ting, and B. Seed. 1998. PPAR-γ agonists inhibit production of monocyte inflammatory cytokines. Nature 391:82–86.
22. Jung, H., T. Kim, H. Z. Chae, K. T. Kim, and H. Ha. 2001. Regulation of macrophage migration inhibitory factor and thiol-specific antioxidant protein PAG by direct interaction. J. Biol. Chem. 276:15504–15510.
23. Kang, S. W., H. Z. Chae, M. S. Seo, K. Kim, I. C. Baines, and S. G. Rhee. 1998. Mammalian peroxiredoxin isoforms can reduce hydrogen peroxide generated in response to growth factors and tumor necrosis factor-α. J. Biol. Chem. 273:6297–6302.
24. Kataoka, K., H. Handa, and M. Nishizawa. 2001. Induction of cellular anti-oxidative stress genes through heterodimeric transcription factor Nrf2/small Maf by antirheumatic gold(I) compounds. J. Biol. Chem. 276:34074–34081.
25. Lee, T. S., H. L. Tsai, and L. Y. Chau. 2003. Induction of heme oxygenase-1 expression in murine macrophages is essential for the anti-inflammatory effect of low dose 15-deoxy-$\Delta^{12,14}$-prostaglandin J_2. J. Biol. Chem. 278: 19325–19330.
26. Metz, C. N., and R. Bucala. 1997. Role of macrophage migration inhibitory factor in the regulation of the immune response. Adv. Immunol. 66:197–223.
27. Narumiya, S., K. Ohno, M. Fukushima, and M. Fujiwara. 1987. Site and mechanism of growth inhibition by prostaglandins. III. Distribution and binding of prostaglandin A_2 and Δ^{12}-prostaglandin J_2 in nuclei. J. Pharmacol. Exp. Ther. 242:306–311.
28. Nathan, C. 2002. Points of control in inflammation. Nature 420:846–852.
29. Negishi, M., T. Koizumi, and A. Ichikawa. 1995. Biological actions of delta 12-prostaglandin J2. J. Lipid Mediat. Cell Signal. 12:443–448.
30. Otterbein, L. E., F. H. Bach, J. Alam, M. Soares, H. Tao Lu, M. Wysk, R. J. Davis, R. A. Flavell, and A. M. Choi. 2000. Carbon monoxide has anti-inflammatory effects involving the mitogen-activated protein kinase pathway. Nat. Med. 6:422–428.
31. Prestera, T., Y. Zhang, S. R. Spencer, C. A. Wilczak, and P. Talalay. 1993. The electrophile counterattack response: protection against neoplasia and toxicity. Adv. Enzyme Regul. 33:281–296.
32. Primiano, T., T. R. Sutter, and T. W. Kensler. 1997. Antioxidant-inducible genes. Adv. Pharmacol. 38:293–328.
33. Ramos-Gomez, M., M. K. Kwak, P. M. Dolan, K. Itoh, M. Yamamoto, P. Talalay, and T. W. Kensler. 2001. Sensitivity to carcinogenesis is increased and chemoprotective efficacy of enzyme inducers is lost in nrf2 transcription factor-deficient mice. Proc. Natl. Acad. Sci. USA 98:3410–3415.
34. Ricote, M., A. C. Li, T. M. Willson, C. J. Kelly, and C. K. Glass. 1998. The peroxisome proliferator-activated receptor-γ is a negative regulator of macrophage activation. Nature 391:79–82.
35. Roger, T., J. David, M. P. Glauser, and T. Calandra. 2001. MIF regulates innate immune responses through modulation of Toll-like receptor 4. Nature 414:920–924.
36. Rossi, A., P. Kapahi, G. Natoli, T. Takahashi, Y. Chen, M. Karin, and M. G. Santoro. 2000. Anti-inflammatory cyclopentenone prostaglandins are direct inhibitors of IκB kinase. Nature 403:103–108.
37. Seibert, K., Y. Zhang, K. Leahy, S. Hauser, J. Masferrer, W. Perkins, L. Lee, and P. Isakson. 1994. Pharmacological and biochemical demonstration of the role of cyclooxygenase 2 in inflammation and pain. Proc. Natl. Acad. Sci. USA 91:12013–12017.
38. Shibata, T., M. Kondo, T. Osawa, N. Shibata, M. Kobayashi, and K. Uchida. 2002. 15-Deoxy-$\Delta^{12,14}$-prostaglandin J_2: a prostaglandin D_2 metabolite generated during inflammatory processes. J. Biol. Chem. 277:10459–10466.
39. Talalay, P., M. J. De Long, and H. J. Prochaska. 1988. Identification of a common chemical signal regulating the induction of enzymes that protect against chemical carcinogenesis. Proc. Natl. Acad. Sci. USA 85:8261–8265.
40. Vane, J. R. 1971. Inhibition of prostaglandin synthesis as a mechanism of action for aspirin-like drugs. Nat. New Biol. 231:232–235.
41. Venugopal, R., and A. K. Jaiswal. 1996. Nrf1 and Nrf2 positively and c-Fos and Fra1 negatively regulate the human antioxidant response element-mediated expression of NAD(P)H:quinone oxidoreductase1 gene. Proc. Natl. Acad. Sci. USA 93:14960–14965.
42. Warner, T. D., F. Giuliano, I. Vojnovic, A. Bukasa, J. A. Mitchell, and J. R. Vane. 1999. Nonsteroid drug selectivities for cyclo-oxygenase-1 rather than cyclo-oxygenase-2 are associated with human gastrointestinal toxicity: a full in vitro analysis. Proc. Natl. Acad. Sci. USA 96:7563–7568.
43. Willis, D., A. R. Moore, R. Frederick, and D. A. Willoughby. 1996. Heme oxygenase: a novel target for the modulation of the inflammatory response. Nat. Med. 2:87–90.
44. Willoughby, D. A., A. R. Moore, and P. R. Colville-Nash. 2000. Cyclopentenone prostaglandins—new allies in the war on inflammation. Nat. Med. 6:137–138.
45. Willoughby, D. A., A. R. Moore, P. R. Colville-Nash, and D. Gilroy. 2000. Resolution of inflammation. Int. J. Immunopharmacol. 22:1131–1135.
46. Yoh, K., K. Itoh, A. Enomoto, A. Hirayama, N. Yamaguchi, M. Kobayashi, N. Morito, A. Koyama, M. Yamamoto, and S. Takahashi. 2001. Nrf2-deficient female mice develop lupus-like autoimmune nephritis. Kidney Int. 60:1343–1353.

Evaluation of MafG interaction with Maf recognition element arrays by surface plasmon resonance imaging technique

Motoki Kyo[1], Tae Yamamoto[2], Hozumi Motohashi[2], Terue Kamiya[1], Toshihiro Kuroita[1], Toshiyuki Tanaka[3], James Douglas Engel[4], Bunsei Kawakami[1] and Masayuki Yamamoto[2,4,5,*]

[1]*TOYOBO Co. Ltd. Bio 21 Project, 10-24 Toyo-Cho, Tsuruga, Fukui 914-0047, Japan*
[2]*Centre for Tsukuba Advanced Research Alliance, University of Tsukuba, 1-1-1 Tennodai, Tsukuba 305-8577, Japan*
[3]*Institute of Applied Biochemistry, University of Tsukuba, 1-1-1 Tennodai, Tsukuba 305-8572, Japan*
[4]*Cell and Developmental Biology, University of Michigan Medical School, Ann Arbor, MI 48109-0616, USA*
[5]*ERATO Environmental Response Project, Japan Science and Technology Corporation, 1-1-1 Tennodai, Tsukuba 305-8577, Japan*

Specific interactions between transcription factors and *cis*-acting DNA sequence motifs are primary events for the transcriptional regulation. Many regulatory elements appear to diverge from the most optimal recognition sequences. To evaluate affinities of a transcription factor to various suboptimal sequences, we have developed a new detection method based on the surface plasmon resonance (SPR) imaging technique. Transcription factor MafG and its recognition sequence MARE (*Maf* recognition elements) were adopted to evaluate the new method. We modified DNA immobilization procedure on to the gold chip, so that a double-stranded DNA array was successfully fabricated. We further found that a hydrophilic flexible spacer composed of the poly (ethylene glycol) moiety between DNA and alkanethiol self-assembled monolayers on the surface is effective for preventing nonspecific adsorption and facilitating specific binding of MafG. Multiple interaction profiles between MafG and six of MARE-related sequences were observed by the SPR imaging technique. The kinetic values obtained by SPR imaging showed very good correlation with those obtained from electrophoretic gel mobility shift assays, although absolute values were deviated from each other. These results demonstrate that the double-stranded DNA array fabricated with the modified multistep procedure can be applied for the comprehensive analysis of the transcription factor-DNA interaction.

Introduction

Specific interactions between transcription factors and *cis*-acting DNA sequence motifs form the molecular basis of the gene expression regulation. Many preceding studies have revealed that one transcription factor usually binds to multiple related *cis*-acting motifs and, conversely, multiple related transcription factors bind to one *cis*-acting DNA motif. However, it has been very difficult technically to identify a specific and important interaction for each transcription factor and *cis*-acting motif. Detailed comparison of the binding affinities between transcription factors and specific *cis*-acting motifs therefore would provide important clue for our understanding of the transcription factor function.

The Maf family proteins appear to be typical members of a large group of regulatory factors characterized by a basic region and leucine zipper (bZip) structure (Motohashi *et al.* 2002). The founding member of this family, v-Maf, is an oncogene, which was discovered as the transforming component of the avian musculoaponeurotic fibrosarcoma virus, AS42 (Nishizawa *et al.* 1989). Subsequently, it was found that the cellular homologue, from which v-Maf was originally transduced (c-Maf), was but one member of a multigene family of related transcription factors. To date, this family consists of four large Maf family members, c-Maf, MafB, NRL, and L-Maf/A-Maf, and three small Maf proteins, MafF, MafG, and MafK (Kataoka *et al.* 1994b, 1995; Swaroop *et al.* 1992; Ogino & Yasuda 1998; Fujiwara *et al.* 1993). The proteins interacting with the small Maf family members have been expanding to include new members in Cap'n'collar (CNC) and Bach families: p45 NF-E2, Nrf1/LCR-F1, Nrf2/ECH, Nrf3, Bach1, and Bach2 (Andrews *et al.* 1993; Chan *et al.* 1993; Moi *et al.* 1994; Itoh *et al.* 1995; Kobayashi *et al.* 1999; Oyake *et al.* 1996). The superficially arbitrary division of the Maf

Communicated by: Shunsuke Ishii
**Correspondence*: E-mail: masi@tara.tsukuba.ac.jp

DOI: 10.1111/j.1365-2443.2004.00711.x

family into small and large members is likely of functional consequence, since all of the large Mafs appear to contain a recognizable transactivation domain, while the small Mafs encode slightly more than the DNA binding and dimerization motifs.

The bZip domain of the Maf factors are characterized by the presence of extended homology region (EHR), which is located in the N-terminal side of the basic region (Swaroop *et al.* 1992; ancillary DNA binding region, Kerppola & Curran 1994). DNA-binding specificity of the Maf family factors was determined by PCR-gel mobility shift assay (GMSA) amplification and purification method (Kerppola & Curran 1994; Kataoka *et al.* 1994a). Conclusion of these studies are that Maf factors recognize relatively long palindromic DNA sequences, $TGCTGA^{G}/_{C}TCAGCA$ and $TGCTGA^{GC}/_{CG}TCAGCA$, which are now known as Maf recognition elements (MAREs). MAREs contain either TPA-responsive element (TRE; $TGA^{G}/_{C}TCA$) or cAMP-responsive element (CRE; $TGA^{GC}/_{CG}TCA$) as a core sequence, and extended elements on both sides of the core sequence (flanking region; 5′-TGC-core-GCA-3′). The recognition of the flanking region in MARE by EHR distinguishes the Maf family proteins from members of the AP-1 or CREB family of the bZip transcription factor superfamily. Kerppola & Curran (1994) showed evidence that the consensus sequence of large Maf binding is $TGC(N)_{6-7}GCA$. Since the flanking region of MARE is consistently required, the study strongly suggests an important contribution of the flanking region to the Maf-specific DNA-binding. Indeed, we showed that Maf EHR is important for the flanking region recognition (Kusunoki *et al.* 2002). It has also been reported through amino acid replacement/mutation analysis that a unique amino acid in the basic region is involved in the flanking region recognition by Maf proteins (Dlakic *et al.* 2001).

Currently, GMSA is a standard method to examine the interaction between transcription factors and DNA motifs and to obtain an equilibrium constant. However, GMSA is a low-throughput method for quantification of the interaction, which usually requires labourious sample preparation steps. Recently, electrodes (Boon *et al.* 2002) and surface plasmon resonance (SPR, Jost *et al.* 1991; Suzuki *et al.* 1998) techniques have been developed, and these techniques are exploited to analyse the interaction between surface immobilized molecules and those in solution. Especially, SPR has advantages that it does not require any labelled reagents and can be applied for the wide surface area (Jordan & Corn 1997). The SPR technique is especially useful for a semiquantitative analysis, as it detects a dynamic real-time interaction profile.

Another recent progress has been made in the field of chip technology, which has been applied for the study of various interactions among proteins and nucleic acid fragments as microarrays (Schena *et al.* 1995; MacBeath & Schreiber 2000; Zhu *et al.* 2001; Bulyk *et al.* 2001; Newman & Keating 2003). Indeed, Nelson *et al.* (1999) developed a prototype of imaging technique for the detection of the biomolecular interaction by combining the SPR and chip technology. This SPR imaging technique seems to enable us to analyse multiple protein-DNA interactions simultaneously and comprehensively. In this respect, SPR is more advantageous than the methods exploiting electrodes upon combination with the chip technology for a comprehensive analysis, since it would be very labourious to construct an array of tiny electrodes on a chip.

Although a multistep array fabrication procedure has been developed for the SPR-chip imaging to detect the protein-DNA interactions (Brockman *et al.* 1999), application of this technology has been hampered due to technical difficulties. In particular, double-stranded DNAs could not be directly immobilized on the chip surface, as organic solvent used in the original procedure easily denatures delicate biomolecules. In the previous procedure (Brockman *et al.* 1999), single-stranded oligonucleotides were first attached on to the gold surface followed by the hybridization with the complementary DNAs to generate double-stranded DNAs on the chip. However, in order to perform a comprehensive affinity quantification of transcription factors to various suboptimal sequences, it is required to fabricate a double-stranded DNA array composed of multiple sequences that are very similar to one another. Immobilization of preannealed double-stranded DNAs is highly preferable for preventing mismatched hybridization and for assuring complete pairing between complementary DNAs.

To develop an efficient and reliable method to detect specific protein-DNA interactions exploiting the SPR technology, we have designed in this study a modified multistep procedure for generation of DNA array on the gold surface, which does not require steps exposing DNA to noxious organic solvents. We also found a better heterobifunctional crosslinker that reduces nonspecific adsorption of the protein to the chip surface in the immobilization process. By utilizing the SPR imaging technique with the newly developed double-stranded DNA array, we then examined binding affinity of MafG, one of the small Maf family members, to several MARE-related DNA sequences. The relative affinities between MafG, various MARE-related sequences showed a very good correlation to those obtained from GMSA. Thus, the new surface immobilization procedure has enabled various delicate biomolecules, including double-stranded

DNAs, to be attached stably on to the gold chip in their native form. This procedure provides a solid basis for the study of SPR-based protein-DNA interactions.

Results

Procedure for immobilization of biomolecules on gold surface

A seven-step fabrication procedure has been used for the immobilization of biomolecules on the gold surface (Brockman *et al.* 1999), which was based on self-assembled monolayers (SAMs) of alkanethiol (Troughton *et al.* 1988; Chidsey & Loiacono 1990) and photolithography technique (Tarlov *et al.* 1993; Huang *et al.* 1994). In the procedure, the hydrophobic protecting group, 9-Fluorenylmethoxycarbonyl (Fmoc), was used for the background protection, and it was deprotected by weak base in organic solvent after single-stranded DNA was immobilized on the surface. In the final step of this procedure, an N-hydroxysuccinimido ester poly(ethylene glycol) (NHS-PEG) was reacted to an amino group on the surface. In these processes, the immobilized single-stranded DNAs were exposed to organic solvents and NHS-PEG.

In order to avoid exposure of test biomolecules to noxious effect, we established a modified procedure to fabricate double-stranded DNA array on the gold surface using thiol-terminated methoxypoly(ethylene glycol), PEG-thiol. This procedure consists of 5 steps described in Fig. 1. Step 1 is the PEG-thiol immobilization on the whole surface area of a gold slide; Step 2 is the photo-patterning by UV irradiation shielded with a bored chromium quartz mask; Step 3 is the introduction of amine terminated alkanethiol on the irradiated spots; Step 4 is the creation of maleimido surface on the spots by reacting with a heterobifunctional crosslinker, which contains a NHS ester and a maleimido group; Step 5 is the 5′-thiol-terminated DNA immobilization by thiol-maleimido coupling reaction.

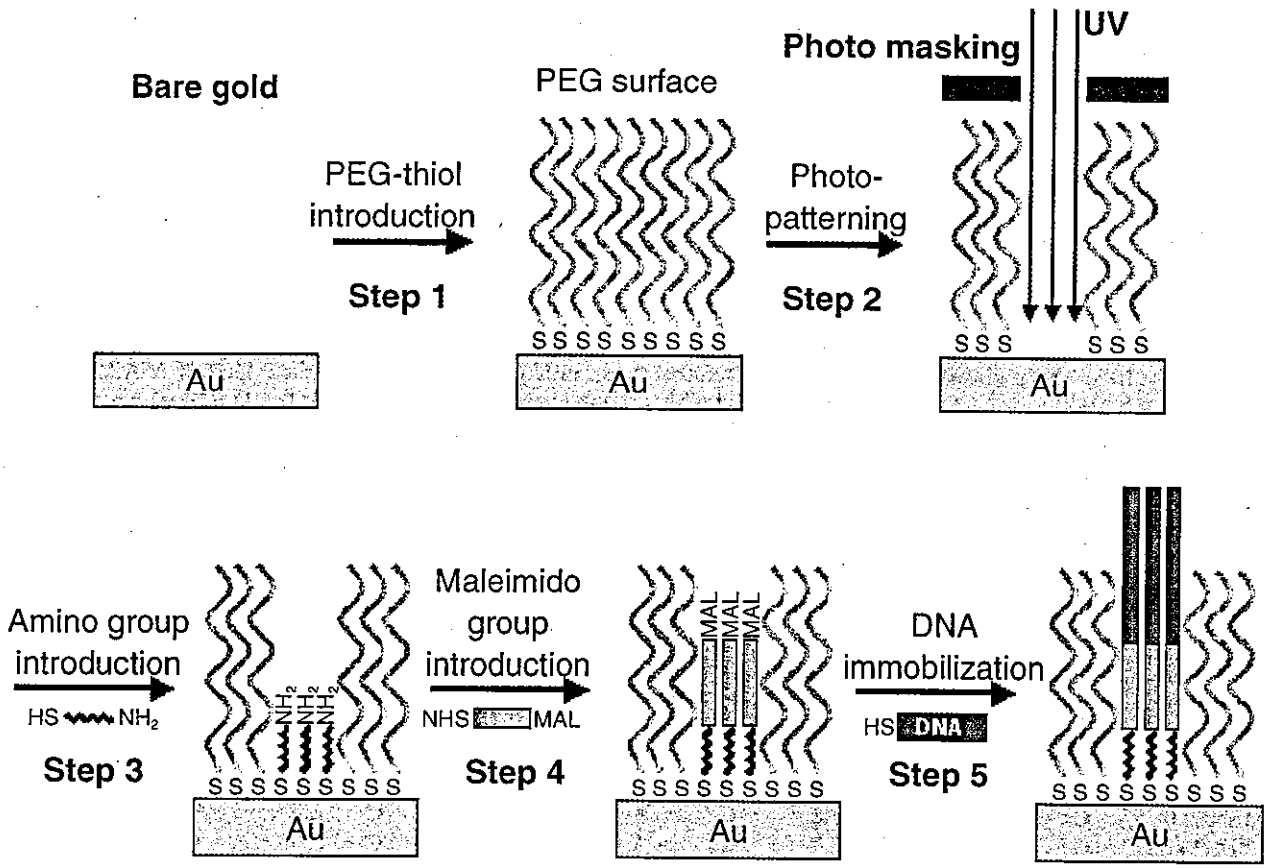

Figure 1 The scheme of surface chemistry to immobilize 5′-thiol terminated DNA. Five steps of DNA immobilization procedure are illustrated. The hydrophilic polymer, PEG-thiol, is first immobilized, which serves as the background of the array (Step 1). DNA spots are created by modifying a self-assembled monolayer of amine terminated alkanethiol, 8-AOT (Steps 2 and 3), with a heterobifunctional crosslinker to prepare a maleimido surface (Step 4). 5′-thiol terminated DNA is added to the spotted region (Step 5).

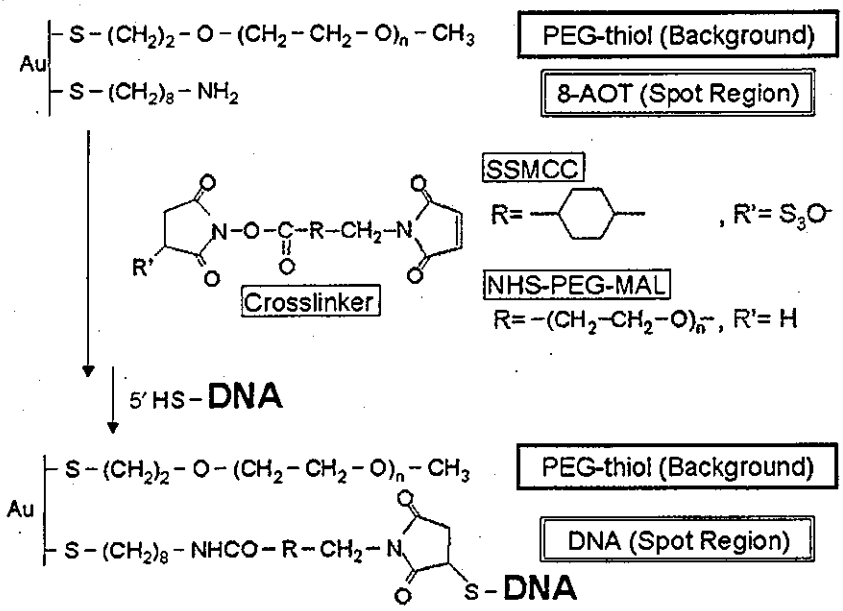

Figure 2 Two different heterobifunctional crosslinkers for specific binding of MafG to DNA array. Two heterobifunctional crosslinkers sulfosuccinimidyl-4-(*N*-maleimidomethyl)cyclohexane-1-carboxalate (SSMCC) and *N*-hydroxysuccinimide-PEG maleimido MW 3400 (NHS-PEG-MAL), were tested for the immobilization of 5′-thiol modified oligonucleotides. SSMCC provides a hydrophobic short linker, while NHS-PEG-MAL possesses a hydrophilic and flexible spacer region.

During these processes, DNA was not exposed to any organic solvents and reagents, since the DNA immobilization was the final step for the array fabrication. Therefore, this modification enabled us to fabricate an array of delicate molecules, such as double-stranded DNAs.

Heterogeneous PEG crosslinker for specific binding of MafG to DNA array

In our effort to establish a standard method for fabrication of a double-stranded DNA array, we also examined the usage of heterobifunctional crosslinkers. Two heterobifunctional crosslinkers, sulfosuccinimidyl-4-(*N*-maleimidomethyl)cyclohexane-1-carboxalate (SSMCC) and *N*-hydroxysuccinimide-PEG maleimido MW 3400 (NHS-PEG-MAL), were tested for the immobilization of 5′-thiol modified oligonucleotides (Fig. 2). SSMCC provides a hydrophobic short linker, while NHS-PEG-MAL possesses a hydrophilic and flexible spacer region.

In comparing the two above-mentioned crosslinkers, we first adopted the sequential DNA immobilization method to assure the generation of double-stranded DNAs on the surface. The reaction scheme to attach DNA on to the chip surface is shown in Fig. 2. 5′-thiol-terminated single-stranded oligonucleotides were first reacted with the maleimido moiety provided by either SSMCC or NHS-PEG-MAL, and the complementary oligonucleotides were hybridized to generate double-stranded DNAs on the surface. Two of MARE-related sequences, MARE25 and MARE23 (Kataoka *et al.* 1994a), were chosen for the assay (Table 1). MARE25 sequence completely matches the consensus sequence for the MafG homodimer binding, while MARE23 sequence has a conserved core region with the altered flanking region.

Table 1 MARE-related sequences for surface immobilization

	5′												3′
MARE25	T	G	C	T	G	A	C	T	C	A	G	C	A
hOPSIN	T	G	C	T	G	A	**T**	T	C	A	G	C	**C**
hNQO1m	**A**	G	**T**	T	G	A	C	T	C	A	G	C	A
MARE23	**C**	**A**	**A**	T	G	A	C	T	C	A	**T**	**T**	G
hBglHS4	**G**	G	C	T	G	A	C	T	C	A	**C**	**T**	**C**
mGSTY	T	G	**G**	T	G	A	C	**A**	**A**	A	G	C	A

The bases different from the MARE25 sequence are in bold. MARE25 contains binding motif that matches the consensus sequence for TRE-type MARE, while MARE23 sequence has a conserved core region with altered flanking region. Flanking sequence of hNQO1 MARE was modified to make the crucial G to be conserved. For this reason we named the DNA as hNQO1m.